Georgia State University
ScholarWorks @ Georgia State University

Chemistry Theses | Department of Chemistry

Summer 7-6-2011

Binding of Bisbenzamidines with AT Rich DNA: A Thermodynamic Study

Nancy A. Kilpatrick
GSU, nkilpatrick1@student.gsu.edu

Follow this and additional works at: https://scholarworks.gsu.edu/chemistry_theses

Recommended Citation
Kilpatrick, Nancy A., "Binding of Bisbenzamidines with AT Rich DNA: A Thermodynamic Study." Thesis, Georgia State University, 2011.
https://scholarworks.gsu.edu/chemistry_theses/41

This Thesis is brought to you for free and open access by the Department of Chemistry at ScholarWorks @ Georgia State University. It has been accepted for inclusion in Chemistry Theses by an authorized administrator of ScholarWorks @ Georgia State University. For more information, please contact scholarworks@gsu.edu.

BINDING OF BISBENZAMIDINES WITH AT RICH DNA: A THERMODYNAMIC STUDY

by

NANCY ANN KILPATRICK

Under the Direction of Dr. W. David Wilson

ABSTRACT

Diamidines are small molecules that generally possess antiparasitic properties and bind preferentially to the minor groove of AT rich DNA. With the goal of getting a better understanding of the thermodynamic driving forces and binding affinities, a series of pentamidine analogs were investigated with various AT rich DNA by ITC, UV-Vis and fluorescence spectroscopic methods. Findings suggest that the substitution of the linker oxygen of pentamidine to a nitrogen slightly improves the binding affinity. All of the investigated compounds are entropically driven at 25 ^{o}C with non-alternating AT DNA. Additionally, the increased fluorescence of the nitrogen and sulfur linked analogs will enable future work to be done with fluorescence microscopy to help determine if and where these compounds accumulate in the target organism.

INDEX WORDS: Binding, DNA, Pentamidine, Minor groove binders, Thermodynamics, ITC

BINDING OF BISBENZAMIDINES WITH AT RICH DNA: A THERMODYNAMIC STUDY

by

NANCY ANN KILPATRICK

A Thesis Submitted in Partial Fulfillment of the Requirements for the Degree of

Master of Science

in the College of Arts and Sciences

Georgia State University

2011

Copyright by
Nancy Ann Kilpatrick
2011

BINDING OF BISBENZAMIDINES WITH AT RICH DNA: A THERMODYNAMIC STUDY

by

NANCY ANN KILPATRICK

Committee Chair: Dr. W. David Wilson

Committee: Dr. Stuart Allison

Dr. David Boykin

Electronic Version Approved:

Office of Graduate Studies

College of Arts and Sciences

Georgia State University

August 2011

DEDICATION

This work is dedicated to my family, without your support this would have never been possible. I gratefully appreciate all the sacrifices everyone in my life has made to see me achieve this accomplishment.

To my mother who never failed to believe in me. You have given your life to your family and in return I give you the credit for helping to mold me into the person I am. Your encouragement has always been a strength to me. From the time I was little, you taught me that I can do anything I set my mind to, no matter the obstacles in my way. And apparently along the way, you managed to fit in teaching me good grammatical skills.

ACKNOWLEDGMENTS

I would like to acknowledge my advisor Dr. W. David Wilson who provided me with the most amazing opportunity in my academic career. I have learned so much from you. You have provided an environment where people can count on each other for support to improve our learning experience.

I would like to thank my committee, who includes Dr. W. David Wilson, Dr. David Boykin and Dr. Stuart Allison, for helping me with this achievement. I would like to particularly thank Dr. Allison for be an amazing teacher who has time and again been there to help me through my studies. I will strive in my life to be as good of teacher as you to those around me.

I would like to acknowledge Carol Wilson for helping proofread my thesis, my CV and cover letters. I am sure my mother will appreciate knowing that she taught me grammar well.

I would like to acknowledge all of my mentors in the lab, especially Dr. Manoj Munde and Dr. Michael Rettig. Manoj, you were patient with me when I was just learning ITC, which took three long months. Michael, you provided me with the support I need, as well as insight into ITC, fluorescence and many other things. I appreciate your ability to share your knowledge and endless editing of my thesis. Thank you very much!

TABLE OF CONTENTS

LIST OF TABLES

LIST OF FIGURES

LIST OF ABBREVIATIONS

A	Adenine
AATT	5’-GCG CAA TTG CGC-3’
ATAT	5’- GCG CAT ATG CGC-3’
A_3T_3	5’-CGA AAT TTC GTC TCC GAA ATT TCG-3’
AAAA	5’-GCG AAA ACG CTC TCG TTT TCG C-3’
C	Cytosine
CCl buffer	Cacodylic Acid Buffer
DNA	Deoxyribonucleic Acid
EDTA	Ethylenediaminetetraacetic Acid
G	Guanine
ΔG	Change in Gibbs’ Free Energy
ΔH	Change in Enthalpy
HCl	Hydrochloric Acid
ITC	Isothermal Titration Calorimetry
K	Binding Constant
N	Nitrogen
NaCl	Sodium Chloride
NaOH	Sodium Hydroxide
O	Oxygen
RT121	1,5-Bis(benzamidine-4-thio)pentane Dihydrochloride
RT124	1,5-Bis(benzamidine-4-sulfonyl)pentane Dihydrochloride
RT394	1,5-Bis(benzamidine-4-amino)pentane Tetrahydrochloride

RT397	1,5-Bis[(N-isopropyl)benzamidine-4-amino]pentane Tetrahydrochloride
RT398	1,5-Bis[4-(2-imidazolinyl)benzene-1-amino]pentane Dihydrochloride
ΔS	Change in Entropy
T	Thymine
T_m	Melting Temperature
ΔT_m	Change in Melting Temperature
UV-Vis	Ultra Violet – Visible
ε	Extinction Coefficient
λ	Wavelength

1 Introduction

The research in this thesis is designed to evaluate the interaction of bisbenzamidines, that have the potential to be therapeutic agents, with an AT rich DNA model system of the trypanosome mitochondrial DNA. It was designed to compare and contrast the fluorescence spectroscopy and thermodynamic properties of binding, such as the binding affinity and the stoichiometry, as well as the binding enthalpic and entropic contributions of pentamidine and analogs when they form complexes with DNA. These studies can provide insight on the driving forces of these biomolecular interactions and aid future drug design.

1.1 Binding: The Center of Biological Cellular Events

"Binding is at the center of all biological cellular events being mediated by a huge array of highly orchestrated, coupled binding reactions."[1] These binding reactions include protein-protein, protein-DNA, protein-RNA, and a host of small molecule-macromolecule interactions.

Quantitative binding studies are able to be performed by a variety of analytical techniques such as calorimetry, spectroscopy and surface plasmon resonance. These methods can determine the distribution of free and bound ligand in a solution. Usually, the raw data is obtained from the technique employed, which must then be analyzed using an appropriate binding model that describes the equilibrium under study.[1]

The goals of binding studies are to answer a series of questions: "How many? How tightly? Why?" The binding study should elucidate the reaction stoichiometry, the affinity of the

binding interaction and the reason the binding is desirable. Some binding studies can also open the door to the actual driving forces of the reaction, the thermodynamics of the binding.

1.2 Thermodynamics

Thermodynamics is the branch of science that describes the behavior of matter and transformation between different forms of energy on a macroscopic level, which include pressure, volume and temperature.[2] As previously stated, thermodynamics can provide information on the driving forces of a reaction; these forces include enthalpy, entropy and the Gibbs free energy.

The enthalpy of a system can be described as the heat absorbed or released, when a reaction occurs at constant pressure. ΔH is a state function, which means that it is independent of the path by which the reaction occurs. However, ΔH is dependent on parameters like temperature and the pressure.[3] A positive ΔH shows that a reaction is absorbing heat during the reaction, while a negative ΔH shows a release of heat. In physical terms, the change in binding enthalpy arises from making, breaking and distortion of bonds within and between the reactant molecules.[4]

The entropy of a system describes the randomness, or disorder associated with that system; it is one measure of the energy distribution of the system.[5] The second law of thermodynamics states that the entropy of the universe is always increasing, or moving towards maximum randomness.[2] A positive ΔS shows an increase in randomness, whereas a negative ΔS shows a decrease in randomness. It is important to note that entropy is not so much a thing as a highly useful mathematical object that provides insight into the change in the reaction, however it is as real as energy or enthalpy. Just like ΔH, ΔS is a state function.[5] In physical terms,

entropy arises from changes in hydration, as well as changes in rotational, translation and configurational freedom. The changes in hydration for a binding reactions are positive and the changes in freedom of movement are generally negative.[6]

Traditionally, biochemist use Gibbs' free energy to describe the energetics of a chemical process. The change in Gibbs' free energy is a measure of the "useful work" that can be done during the course of a reaction.[3] The sign of ΔG shows whether a reaction under given conditions is spontaneous, or not. A negative ΔG shows that a particular reaction is spontaneous, whereas a positive ΔG is nonspontaneous. ΔG, which encompasses both enthalpy and entropy, is given by:

where ΔG is the change in Gibbs' free energy, ΔH is the change in enthalpy, T is the temperature and ΔS is the change in entropy.[2] Additionally, ΔG can be related to the binding constant for a reaction in equilibrium by:

where ΔG^0 is the change in Gibbs' free energy at the standard state, R is the molar gas constant (8.314 J K^{-1} mol^{-1}), T is temperature and K is the binding constant.[2]

1.3 DNA-Small Molecule Binding

There are two major classes of binding for DNA-small molecule interactions: covalent and non-covalent. Covalent interactions usually involve a permanent change in nucleic acid structure, where noncovalent interactions are reversible. Covalent binding can take place on the phosphodiester backbone or sugar residues, as well as bases.[7] Noncovalent interactions include

electrostatic, hydrophobic and van der Waals interactions, as well as base stacking and hydrogen bonds.[8]

It is believed that a large number of important drugs and antibiotics exert their primary biological action by means of noncovalent interactions with DNA, subsequently inhibiting the template functions of transcription and replication. Activity for many of these compounds have been shown to work against a large number of human and animal diseases, ranging from cancer, bacterial infections, viral infections and parasitic diseases, such as malaria and trypanosomiasis.[7]

There are three main modes of noncovalent interaction for DNA and small molecules, which include external binding, groove binding and intercalation. External binding involves a ligand binding to the outside of the helix through non-specific electrostatic interactions with the sugar-phosphate backbone. In groove binding, the ligand makes direct molecular contacts with the functional groups on the edges of the bases that protrude into the major or minor groove, whereas intercalation occurs in between adjacent base pairs (Figure 1.1).[8] Two individual intercalators can be linked together to form a bis-intercalator.

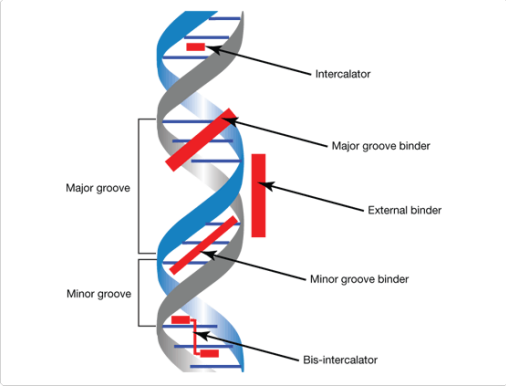

Figure 1.1 Schematic of primary noncovalent binding modes for DNA and small molecules. (http://www.invitrogen.com/site/us/en/home/References/Molecular-Probes-The-Handbook/Nucleic-Acid-Detection-and-Genomics-Technology/Nucleic-Acid-Stains.html#head1)

1.4 Minor Groove as a Target for Binding

A large family of diverse compounds can be classified as DNA groove binders. Most of the compounds have shown biological activity for use as antiparasitic and antiviral agents. They generally show a preference for binding the AT rich regions of DNA and almost exclusively for the minor groove of B-form DNA.[7] This is typified by the antitrypanocidal agents berenil and pentamidine.

There are several structural features common to DNA minor groove binding compounds. The compounds are generally positively charged. The molecule is linked, rather than having fused aromatic or heteroaromatic rings.[7] These molecules are typically composed of several aromatic rings, such as pyrrole, furan or benzene that have bonds that possess torsional freedom.[9] The shape of a classical minor groove binder is crescent shaped and closely fits the helical twist of the minor groove of DNA.[10]

The minor groove is narrower than the major groove in B-form DNA, 6.0 Å and 11.6 Å respectively. The narrower dimensions of the minor groove are more amendable to small molecule binding, whereas the major groove is more suited to the binding of larger molecules, such as proteins.[11] The ligands generally bind with the aromatic groups of the ligand lying between and parallel to the two sugar-phosphate backbones. Typically, the ligands that bind to the minor groove of DNA are in the AT rich region. This preference is due to several factors. There are favorable hydrophobic contacts between the adenine C2 hydrogen atoms and the aromatic rings in the ligand. As well, the AT base pairs possess hydrogen bond acceptors at the C2 carbonyl oxygen of thymine and N3 nitrogen of adenine, which can interact with hydrogen bond donors of the ligand. There is steric hindrance for the ligand to bind to GC sequences due

to the exocyclic amino group on the guanosine.[9] In the AT rich regions, the minor groove tends to be narrower than GC regions and atoms forming the backbone and groove floor are in close van der Waals contact with the ligand.[7]

1.5 Diamidines

Diamidine are a class of compounds characterized by having amidine groups at the terminal ends of the molecule, with varying intervening groups. Diamidines are known to bind to 4 to 5 base pairs in the minor groove of DNA. Typically, the amidine groups hydrogen-bond to the C2 carbonyl oxygen of thymine, or the N3 nitrogen of adenine on the floor of the minor groove.[12] Typically, diamidines bind 100 or more times more weakly to GC containing sequences, rather than to pure AT sites.[10] This binding affinity gives diamidines a preference for AT rich sites. Two well-known diamidines drugs are pentamidine and berenil.

1.5.1 Pentamidine

Pentamidine is a bisbenzamidine derivative (Figure 1.3) currently used to treat eukaryotic parasitic induced diseases, such as trypanosomiasis (sleeping sickness), leishmaniasis, and *P. carinii* pneumonia.[10] Pentamidine was introduced in the 1940s.[13] The mechanism of action of pentamidine is not known, due in part to the fact that pentamidine does not fluoresce. However, x-ray crystallography has shown that pentamidine is a DNA minor groove binder (Figure 1.2).[14]

As stated above, pentamidine has been shown to bind to the minor groove of the DNA duplex CGCGAATTCGCG. The pentamidine symmetrically spans over the four AT base pairs. The cationic terminal ends are positioned deep in the groove, rather than close to the negatively charged phosphate groups. Pentamidine directly hydrogen bonds to the DNA between the amidinium groups of the drug to N3 of A5 and N3 of A17 on the opposite strand. Additionally,

there are close contacts to the deoxyribose O4' atoms of A6 and A18, together with a water-mediated contact of O4' of G10. The two phenyl rings of the bound pentamidine are twisted 35^{o} with respect to each other, causing the rings to be parallel to the walls of the groove and follow the curvature of the DNA. The phenyl rings contact the floor of the minor groove.[14]

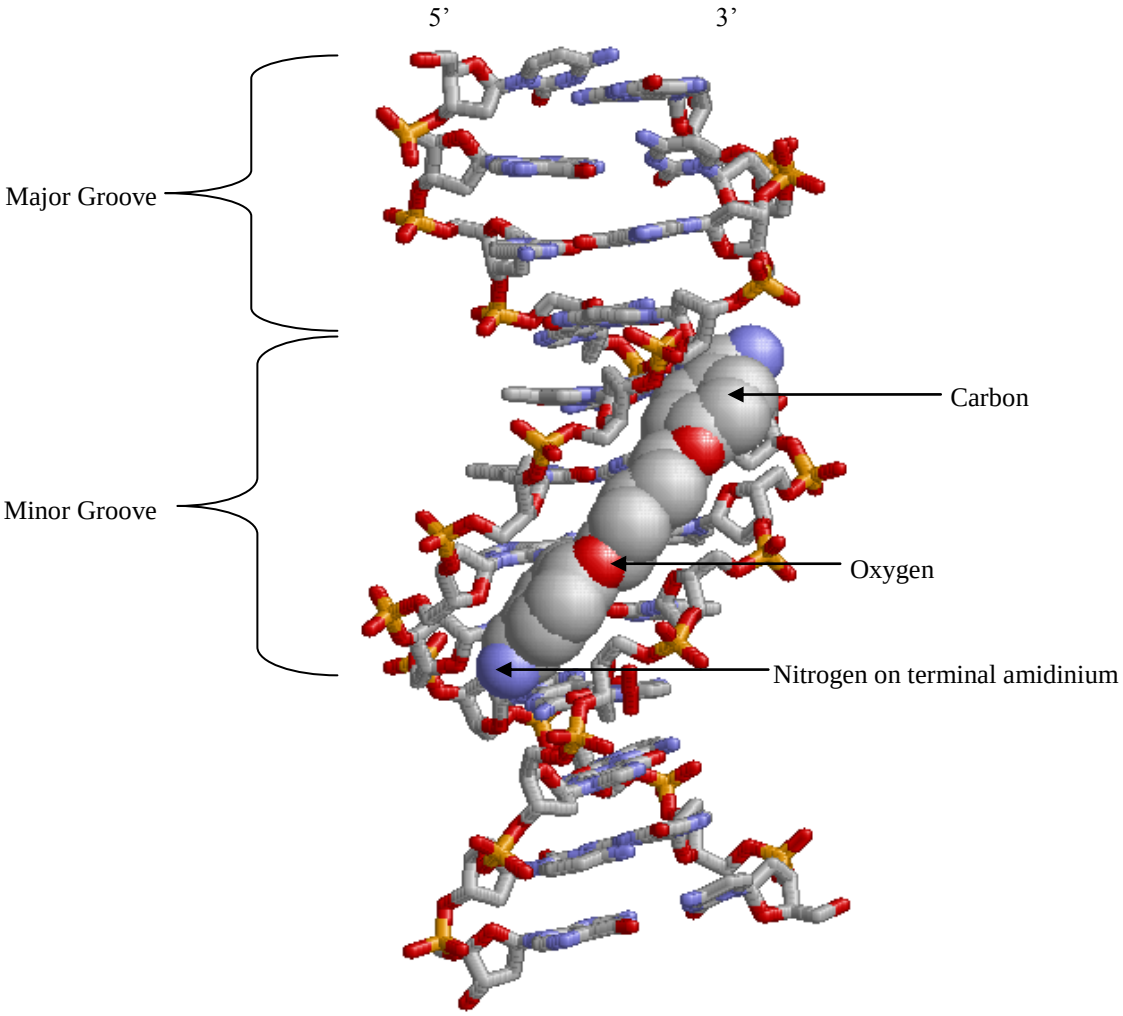

Figure 1.2 The crystal structure of the complex formed between the DNA duplex CGCGAATTCGCG and pentamidine. Pentamidine is bound in the minor groove of the DNA duplex, specifically the AATT site. The amidinium nitrogen atoms form hydrogen bonds with the A5 on one strand and A17 of the second strand. Additionally, A6 and A18 are in close contact with the deoxyribose O4'. In the diagram, gray atoms are carbon, blue atoms are nitrogen, red atoms are oxygen and yellow atoms are phosphate.

Pentamidine has been curing people with African trypanosomiasis and leishmaniasis for nearly 70 years, without the development of drug resistant strains. Recently, during the HIV/AIDS epidemic, it has been used to treat AIDS-related *P.carinii* pneumonia.[10] However, there are inherent problems that warrant the discovery of new compounds. Pentamidine is protonated at physiological pH and is not able to be administered orally. This is a problem because many of the people that are affected with these diseases are usually in Africa where it is difficult and costly to get multiple injections. Additionally pentamidine is only a treatment for the early phase of the sleeping sickness, because it does not cross the blood brain barrier, where the late phase of the disease occurs.[13] Another issue is the toxicity of pentamidine; toxic side effects include abscesses at the injection site, abnormal liver function, hypotension, nephrotoxicity, cardiotoxicity and hypoglycemia.[10]

1.5.2 Pentamidine Analogs

Pentamidine was used as a molecular template due to its established clinical efficacy. The pentamidine analogs used were chosen to systematically test the effects of changing the oxygen in the linker region, as well as different N-substitutions on the cationic fragments on binding affinity with the DNA minor groove (Figure 1.3). One of the compounds, RT121, has the oxygen linkers replaced with sulfur. RT124 has the oxygen linkers replaced with the larger sulfonyl molecules. RT394, RT397 and RT398 have the oxygen linkers replaced with nitrogen linkers. In a recent *in vivo* mouse study of pentamidine analogs, the replacement of oxygen with nitrogen showed a decrease in toxicity to the mouse.[15] In addition to the change in the linker, RT397 and RT398 have a substitution on the terminal amidinium groups of an isopropyl and imidazoline rings, respectively.

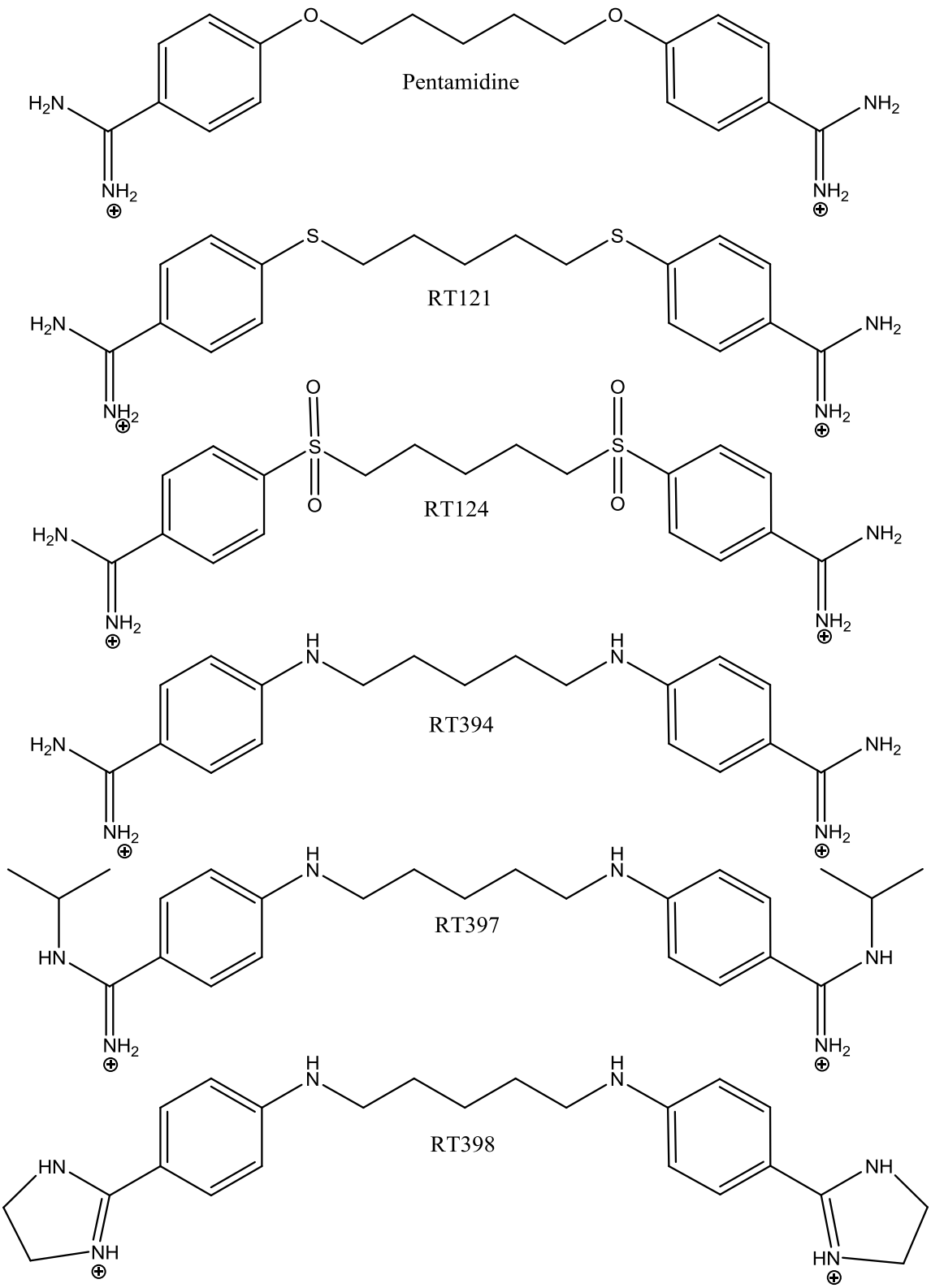

Figure 1.3 Pentamidine and analogs structures synthesized by the laboratory of Dr. Richard Tidwell, University of North Carolina at Chapel Hill.

In molecular modeling studies, it has been shown that pentamidine analogs bind to the DNA minor groove similarly to pentamidine. The phenyl groups are aligned to be parallel to the walls of the minor groove and the amidinium groups are twisted out of the plane of the phenyl rings. The linker modification of oxygen to nitrogen has indicated a ~ 0.5 base pair shift relative to pentamidine. This shift facilitates increased van der Waals contacts with the minor groove and results in strong hydrogen bond contact with the deoxyribose oxygen acceptors.[16]

Recent biological studies, with the compounds and *T.b. rhodesiense, P. falciparum,* and *L. donovani*, have shown that all of these compounds are biologically active. In the in vitro study, the cytotoxicity to the parasites was decreased for the sulfur analogs and increased for the nitrogen analogs in comparison to pentamidine. Furthermore, the terminal amidinium substitution for RT397 and RT398 showed a decrease in cytotoxicity compare to the unsubstituted RT394. The RT compounds had increased selectivity of the parasite DNA as compared to the L6 cell line. Notably, RT398 was more selectivity for *T.b. rhodesiense, P. falciparum,* and *L. donovan* than pentamidine by 64, 127 and 68 times, respectively. However, the in vivo studies of mice infected with trypanosomiasis, RT121 and RT397 were inactive and RT394 had a 1 out of 4 cure rate. Remarkably, RT398 provided a cure for all infected mice.[15]

1.6 General Methods

1.6.1 Absorbance Maximum and Extinction Coefficient

Many compounds absorb light in the ultra-violet and visible range from 10-400 nm and 400-700 nm, respectively. The extinction coefficient of a known concentration of a compound can be determined from the absorbance at its maximum wavelength. Beer's Law states that the absorbance of a compound is directly proportional to the concentration of the absorbing species

and the pathlength. The extinction coefficient is a property of the molecule undergoing an electronic transition. The larger the extinction coefficient the greater the probability that the electronic transition will take place.[17]

1.6.2 Thermal Melting

DNA typically exists as two single strands arranged in a double helix by complementary base pairing of AT and GC. The AT base pairs have two hydrogen bonds, whereas the GC base pairs have three hydrogen bonds. If the temperature of a DNA solution is raised sufficiently, the DNA can be melted, or denatured.[18] Denaturation is the dissociation of this helix into two single stranded random coils.

Among the factors contributing to the overall DNA double helix structure, there are two factors that play a significant role in the transition from the DNA double helix to two single stranded random coils. The first is the electrostatic repulsions of the two strands in the helix, since DNA carries a negative charge on each phosphate group at physiological pH. The negative charge is partially neutralized by the small counterions, such as Na^+, K^+ and Mg^{2+}, but a substantial charge remains and the two strands are driven apart.[19] When the salt concentration is low the repulsion is larger, however as the salt concentration increases, the repulsion decreases. Typically, a salt concentration greater than 1M affects the ability of the bases to hydrogen bond, thus decreasing stability. [20,21] The second factor is the gain in entropy by converting one double stranded DNA helix into two single stranded random coil structures.[19]

The $\Delta G_{denaturation}$ is initially positive at a temperature below the melting point, whereas it turns negative for the temperature above it. The $\Delta G_{denaturation}$ is determined by equation 1.1. As stated above, the entropy contribution is favorable for the denaturation; ΔS is positive.[19] On the

other hand, the breaking of hydrogen bonds between the two strands of DNA, a loss of van der Waals contacts and changes in hydration, lead to an unfavorable ΔH for the melting process. As the temperature is increased, the ΔS term makes a greater contribution and overcomes the ΔH contribution, at this point $\Delta G_{denaturation}$ is negative. Once the $\Delta G_{denaturation}$ is negative, the two strands will fall apart, or melt. This change occurs over a very narrow temperature range, since the whole structure holds together until it is at the verge of instability.[19]

It is possible to monitor this denaturation, or melting, process by observing the absorbance of ultraviolet light at 260 nm in a DNA solution.[18] DNA absorbs light strongly in this region. When the DNA is packed into a double stranded helix the DNA absorbs less light; this is called hypochromism. Once the secondary structure is lost and the DNA melts into two single strands, the light absorbance increases. Therefore, upon increasing the temperature of the DNA solution and the subsequent loss of secondary structure, this will result in a change in absorbance, as shown in Figure 1.4.[19] During this transition from a double stranded helix to two single stranded random coils, the midpoint is defined as the melting temperature, T_m. At the T_m, half of the DNA exists in the double stranded helical state and the other half exists in the single-stranded state and the two species are in equilibrium.[18] The T_m can be determined by using the first derivative of the melting curve. At the T_m the first derivative equals zero.

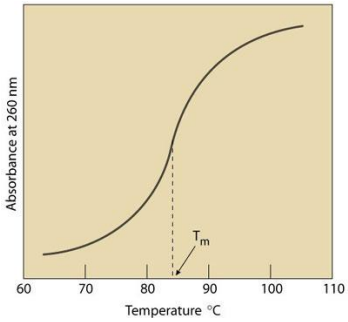

Figure 1.4 Sample of a thermal melting curve for DNA.
(http://www.doctortee.com/dsu/tiftickjian/genetics/dna.html)

The stability of the DNA double helix is found to increase as the GC base pair content increases. This is due to the increased number of hydrogen bonds and increased base stacking in GC base pairs over AT base pairs. Another factor in increased stability is ligand binding. If a ligand binds and increases the stability of the double helix, the melting temperature will increase.[18]

1.6.3 Isothermal Titration Calorimetry

Isothermal titration calorimetry can provide a complete thermodynamic profile of a binding reaction. This thermodynamic profile consists of free energy, enthalpy, entropy and reaction stoichiometry. These profiles are valuable in drug design because they provide quantitative data on the driving forces that cannot be obtained by structural or computational methods alone.[22] Additionally, these profiles can be used for the evaluation and understanding of substituent changes on binding affinity.

ITC measures the energetics of a biochemical or molecular interaction at a constant temperature. The ligand is sequentially titrated to completion under conditions that allow for the extraction of thermodynamic properties that define the binding process.[23] The observed quantity during the experiment is the heat absorbed or released upon the injection of the ligand into the sample cell. The system monitors the temperature difference between the sample cell and the reference cell as the ligand is injected. Any heat of the binding reaction causes an imbalance between the sample cell and reference cell, which is compensated for by modulating the power applied to the sample cell to regain the same temperature as the reference cell.[22] Exothermic reactions will temporarily decrease and endothermic reactions will temporarily increase the

feedback power. The reaction heats are obtained by the computer integration of the changes in power from the resting baseline.[24]

Representative ITC data is shown in Figure 1.5. The top panel shows the primary data recorded for the experiment in which power applied to the sample cell is displayed as a function of time for each injection. The area of each peak reflects the heat of the reaction for each reactant injection. The quantity of heat absorbed or released is directly proportional to the amount of binding, when $\Delta H \neq 0$.[23] The bottom panel shows the integration of the primary data into the binding isotherm. The binding isotherm is fit to a particular binding model using a nonlinear least-squares analysis to obtain a binding constant, enthalpy and binding stoichiometry.

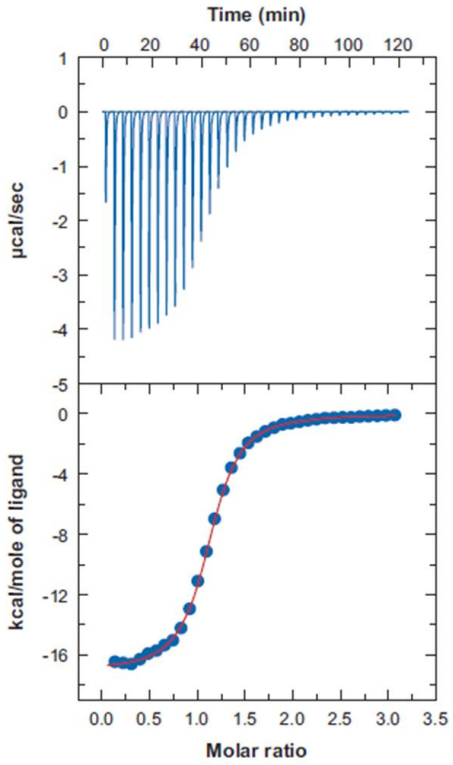

Figure 1.5 Representative ITC curve. The ITC raw data, located in the top panel, is the power output per injection as a function of time. The bottom panel is the peak integration of the data that shows the heat produced per injection as a function of the DNA/ligand molar ratio.

The independent variables are the ΔH, the single-site binding constant (K), and the reaction stoichiometry (n). The dependent variables are ΔG and ΔS. ΔG is calculated by:

where ΔG^0 is the change in Gibbs' free energy at the standard state, R is the molar gas constant (8.314 J K^{-1} mol^{-1}), T is temperature and K is the binding constant.[2] ΔS is calculated by:

---

where ΔS is the change in entropy, ΔH is the change in enthalpy, ΔG is the change in Gibbs' free energy and T is the temperature.[24]

It is important to understand the contributions of enthalpy and entropy to the overall free energy. The ΔH is the heat associated with the making and breaking of non-covalent bonds going from the free to the bound state.[25] Bearing in mind, when a hydrogen bond is made between biomolecules, it often replaces bonds that were previously made with solvent water, thereby the net enthalpy is reduced by the desolvation. The ΔS reports on the overall change in degrees of freedom of the system. This can be due in large part to the effect of liberating water molecules from the surface of the ligand, as well as release of water molecules from the DNA , upon binding.[25]

ITC has several advantages to other techinques, such as spectroscopic methods, to determine reaction binding constants. Not only does ITC determine the binding constant, it is the only way to obtain a complete thermodynamic profile of a reaction in one experiment, from its unique ability to measure heat directly. The heat signal that is obtained is generally a

universal property of binding reactions, so it is applicable to most macromolecule-ligand interactions, whereas for fluorescence methods the ligand must contain a chromophore, or be labelled to produce a signal that can be measured by that method.[24] Additionally, ITC is a true in solution method that does not require immobilization of interacting components or chemical modification.[25]

1.6.4 Fluorescence

Fluorescence titration allows for quantitation of ligand binding affinity under equilibrium conditions.[26] However, an appropriate binding model must be selected to fit the titration results and this requires the binding stoichiometries be determined. Binding stoichiometries can be determined by a Job's plot using fluorescence, UV, or cicrcular dichroism. Alternatively, stoichiometry can be determined by ITC, as was done in this study.

Molecules containing a chromophore can fluoresce. The fluorescence of a molecule is effected by its local environment. When a ligand interacts with DNA, it may cause a change in fluorescence, either an increase or decrease. Using appropriate experimental conditions, this change in fluorescence is directly related to the ligand concentration, since DNA does not fluoresce.[27]

There are several advantages of fluorescence based methods. The high sensitivity of the instrument allows for micromolar or lower sample concentrations, thus relatively small amounts of DNA and ligand are needed. Since it is a solution method, it is amenable to varying solutions conditions, such as pH, ionic strength and temperature.[27]

The lack of fluorescence of pentamidine prevents microscopy studies, which could determine its localization. DB75 is a known antitrypanosomal diamidine compound that binds to

AT rich DNA. DB75 has intense fluorescence, unlike pentamidine. In previous studies, the DB75 was studied with fluorescence microscopy, in which it was shown to accumulate in the DNA-containing nucleus and the kinetoplast in the mitochondria of the trypanosome.[28]

1.7 Research Objectives

The goals of this research are to determine whether the pentamidine analogs show fluorescence that could be used in cellular and biophysical studies. Specific points to address in this research are:

(i.) Do these analogs increase or decrease in fluorescence upon binding with DNA?

(ii.) Is the fluorescence intensity of the analogs enough so that future work can be done with fluorescence microscopy to help determine where these compounds go in cells?

(iii.) Does the substitution in the linker of pentamidine have an effect on the binding affinity with AT rich DNA?

(iv.) Furthermore is binding affinity affected upon changing the linker to nitrogen and substitution on the terminal amidinium group?

(v.) Is the binding reaction driven enthalpically or entropically?

(vi.) Does the binding affinity of these compounds change between alternating and non-alternating AT sequences?

(vii.) Can the results from this research give insight in to the result of the previous biological studies?

2 Experimental

2.1 Cacodylic Acid Buffer Preparation

The buffer was prepared with deionized water to a final volume of 1L containing 100 mmol NaCl, 10 mmol Cacodylic acid and 1 mmol EDTA (Fisher Scientific, Fair Lawn, NJ). The buffer was heated gently and stirred until completely dissolved for approximately one hour. The pH was adjusted to 6.25 by drop wise additions of 1N NaOH (EM Science, Gibbstown, NJ).

2.2 Preparation of DNA Oligomers

The DNA oligomers were all prepared based on the estimated moles from the manufacturer; the lyophilized DNA had the appropriate amount of deionized water added to make an estimated concentration of 1 mM. The DNA was annealed by placing it in a beaker of boiling water that had been removed from the heating source. The DNA was allowed to remain in the beaker of water until it had cooled to room temperature.

The final concentration was determined by using the Cary 300 UV-Vis Spectrophotometer with the Cary 300 Win UV Simple Reads application (Varian, Inc., Palo Alto, CA). The wavelength was set to 260 nm. The instrument was zeroed with a 1 cm pathlength cuvette containing 997 μL of water. Then, 3 μL of DNA was added to the same cuvette. The absorbance of the DNA was measured three times. The instrument was zeroed again, while leaving the cuvette in the transport. An additional 3 μL of DNA was added to the same cuvette. The absorbance of the DNA was measured three more times. Using the average absorbance, the molar extinction coefficient of the compound was calculated from Beer's Law:

where A is absorbance, ε is molar extinction coefficient, c is concentration and b is the pathlength. The molar extinction coefficient was provided by the manufacturer of the DNA. The actual concentration of the original stock DNA was determined by:

$$\frac{\qquad\qquad}{\qquad\qquad}$$

where M is concentration and V is volume.

The DNA oligomers AATT, AAAA and ATAT were obtained from Integrated DNA Technologies (Coralville, IA). The DNA oligomer A_3T_3 was obtained from Midland Certified Reagent Company (Midland, TX). The DNA oligomer Poly(dA)•Poly(dT) was obtained from Amersham Biosciences (Piscataway, NJ).

2.3 Preparation of DNA Binding Ligands

A 1mM solution was prepared for each of the compounds by weighting out the appropriate amount of the compound on an analytical balance and adding the corresponding volume of deionized water by pipette. The solution was stirred until the solid had dissolved. If necessary, the solution was gently heated, so as not to boil, to aid in the compound dissolving.

The compounds RT121, RT124, RT394, RT397, RT398 and pentamidine were synthesized by the laboratory of Richard Tidwell at the University of North Carolina (Chapel Hill, NC).

2.4 Determination of Absorbance Maximum and Extinction Coefficient

The experiments were performed on a Cary 300 UV-Vis Spectrophotometer with the Cary 300 Win UV Scan application. A 10 μM solution of compound in deionized water was placed in a 1cm pathlength cuvette. To determine the absorbance maximum of the compound, the sample was scanned from 400 nm to 250 nm at a rate of 60 nm per minute. This was repeated two more times. The averaged maximum absorbance was used to calculate the estimated extinction coefficient of the compound in the cuvette using the equation 2.1.

To determine an accurate molar extinction coefficient, a UV-Vis titration was performed for the compound at its absorbance maximum as defined before. The compound was titrated into the cuvette for various concentrations corresponding to an absorbance of 0.1 to 0.8 based on the estimated molar extinction coefficient. The data was plotted for absorbance as a function of concentration, therefore the slope of the graph is the extinction coefficient multiplied by the pathlength, which was 1 cm.

2.5 Thermal Melting

The compound and DNA were placed in a 1 cm pathlength cuvette according to the following ratios. A molar ratio of 2:1 (compound to DNA) was used for AATT, A_3T_3 and AAAA. The ratio of 0.5 per base pair of DNA and 1.0 per base pair of DNA (compound to DNA) was used for Poly(dA)•Poly(dT).

The thermal melting experiments were performed on the Cary 300 UV-Vis Spectrophotometer using the Cary Win UV Thermal Melting application. The instrument was zeroed with no reference. The method to collect the data was to ramp the temperature from 25 ^{o}C to 95 ^{o}C at a rate of 0.5 ^{o}C per minute. Once a 95 ^{o}C temperature had been reached the

temperature was held for 10 minutes. The temperature was then ramped to 25 ^{o}C at a rate of 0.5 ^{o}C per minute. Once a 25 ^{o}C temperature had been reached the temperature was held for 10 minutes. The temperature was then ramped to 95 ^{o}C at a rate of 0.5 ^{o}C per minute. The derivative of the graph was used to determine the melting temperature using the Cary 300 Win UV software.

2.6 Isothermal Titration Calorimetry

A 20 μM DNA solution was prepared with CCl buffer. A 200 μM ligand solution was prepared with CCl buffer. The solutions were stirred and degassed for 15 minutes at the appropriate temperature for the experiment.

The experiments were performed on the Microcal^{TM} VPC-ITC (Microcal^{TM} part of GE Healthcare, Northampton, MA). The VPC-ITC sample cell and syringe were thoroughly cleaned. The DNA solution was placed in the sample cell, approximately 1.4 mL. The ligand solution was placed in the injection syringe, approximately 300 μL. The reference cell contained degassed buffer, approximately 1.4 mL. The typical experimental parameters in the VPViewer 2000 software were set to 30 total injections, a cell temperature of 25 ^{o}C, a reference power of 1 μcal/sec, an initial delay of 300 sec, syringe concentration of 200 μM, cell concentration of 20 μM and stirring speed of 290. The feedback mode/gain was high. The ITC equilibrium options were set for fast and auto. The injection parameters for the 1st injection were 2 μL volume, duration of 4 sec, a spacing of 300 sec, and a filter period of 1 sec. The remaining injections were set to 10 μL volume, duration of 20 sec, a spacing of 300 sec, and a filter period of 1 sec.

The entire procedure was repeated for baseline adjustment data, with the following alteration: the sample cell contained buffer only, with no DNA. This was used to adjust results for the compound interaction with the buffer.

The data was analyzed with Origin 7.0 (Microcal^{TM} part of GE Healthcare, Northampton, MA) using a single site binding model. For a detailed description of the ITC procedures refer to the Appendix.

2.7 Fluorescence

The DNA solution was prepared at a concentration of 500 μM in CCl buffer. The DNA binding ligands were prepared at a concentration of 1 mM in CCl buffer.

The fluorescence titrations were performed using Cary Eclipse Scan (Varian, Inc., Palo Alto, CA 94304). The scan was setup for the maximum excitation λ of the ligand. The scan was started 20 nm higher than the excitation λ and scanned an additional 200 nm beyond that. The excitation and emission slit widths were 5 nm. The scans were overlaid for analysis. The 1 cm pathlength cuvette with 985 μL of buffer was placed in the instrument to zero it. After the instrument was zeroed, 1 μL DNA binding ligand was added to the cuvette. The cuvette was placed in the instrument and scanned. After the baseline scan, 1 μL of 500 μM AATT was added to the same cuvette and scanned. The AATT was added until saturation was achieved.

The data was analyzed with Origin 7.0 using a single binding site model. To determine K, plot the normalized fluorescence versus the DNA concentration and perform a non-linear least squares regression with K and η as fitting parameters. As given by:

Where F is the observed fluorescence, L_0 is the total ligand concentration, is the molar fluorescence of the free ligand, K is the equilibrium binding constant, [M] is the free DNA concentration and is the fluorescence enhancement factor. Equation (2.3) can be reduced to:

where, $[M_0]$ and $[L_0]$ are the total concentration of the DNA and the total concentration of ligand, respectively and K is the equilibrium binding constant. By solving the quadratic in equation 2.4 with total DNA concentration $[M_0]$ it gives you free DNA concentration [M]. [29]

3 Results

3.1 Absorbance Maximum and Extinction Coefficient

The maximum absorbance was used to determine the molar extinction coefficient (ε) by Beer's Law. Beer's Law states that $A = \varepsilon bc$, where A is absorbance, ε is molar extinction coefficient, b is pathlength of the cuvette, and c is concentration.[30] The molar extinction coefficient and maximum wavelength for the compounds are shown in Table 3.1. The maximum wavelength and extinction coefficient determined for pentamidine was 261.0 nm and 28,700 M^{-1} cm^{-1}, respectively, which is consistent with the literature values of 262 nm and 28,900 M^{-1} cm^{-1}.[31] The molar extinction coefficients for RT394, RT397 and RT398, which have nitrogen linkers, are higher than pentamidine, as are the λ_{max} values. RT121, which has a sulfur linker, has a comparable molar extinction coefficient to pentamidine. In contrast, RT124, which has a sulfonyl linker, has an extinction coefficient of 4090 M^{-1} cm^{-1}, which is significantly lower than pentamidine.

Table 3.1 Absorbance maximum and extinction coefficient for pentamidine analogs in deionized water at 25 ^{o}C.

Ligand	λ (nm)	ε (M^{-1} cm^{-1})
Pentamidine	261.0	28,700
RT121	296.9	34,300
RT124	274.9	4,090
RT394	315.8	55,400
RT397	306.5	53,600
RT398	322.9	76,800

3.2 Thermal Melting

The T_m values for the individual duplex and polymeric DNA sequences used in this research are shown in Table 3.2. In general, the T_m values increased with increased length of AT site in the various DNA sequences for the investigated compounds. The investigated compounds all had similar ΔT_m values for the AATT sequence, whereas the ΔT_m values varied for all the other sequences, as shown in Table 3.3. For the A_3T_3 sequence, compounds RT394, RT397, and RT398 showed a slightly higher increase in thermal melting temperature than pentamidine. Interestingly, when changing the AT site from A_3T_3 to AAAA, pentamidine showed a 1 ^oC ΔT_m, while RT394, RT397, and RT398 did not change the T_m at all. The most significant changes in T_m were seen with the polymeric DNA. The ΔT_m value for RT121 and the Poly(dA)•Poly(dT) sequence was the highest, followed by pentamidine. RT124 and Poly(dA)•Poly(dT) showed the lowest increase in ΔT_m. The ΔT_m values for nitrogen linked compounds (RT394, RT397 and RT398) and Poly(dA)•Poly(dT) were similar, but slightly less than those for pentamidine. The increased ratio from 0.5 to 1 for the Poly(dA)•Poly(dT) only showed a minor change in ΔT_m. The error for the change in thermal melting temperature for duplex DNA is ± 1 ^oC and for the polymer DNA is ± 0.5 ^oC.

Table 3.2 Thermal melting temperature for DNA oligomers.

DNA	**T_m (^{o}C)**
AATT	43.5
A_3 T_3	67.0
AAAA	72.0
Poly(dA)·Poly(dT)	68.05

Table 3.3 Changes in thermal melting temperatures for investigated ligand-DNA complexes. Indicated ratios represent ligand to DNA duplex and ligand to base pair for oligomers and polymeric DNA, respectively.

	ΔT_m (^{o}C)				
	2:1	**2:1**	**2:1**	**0.5:1**	**1:1**
	AATT	**A_3 T_3**	**AAAA**	**Poly(dA)·Poly(dT)**	**Poly(dA)·Poly(dT)**
Pentamidine	1	2	1	11.1	13.1
RT121	2	-	-	-	16.9
RT124	1	-	-	-	10.0
RT394	1	3	0	9.0	12.0
RT397	1	3	0	8.8	11.1
RT398	1	4	0	10.6	12.2

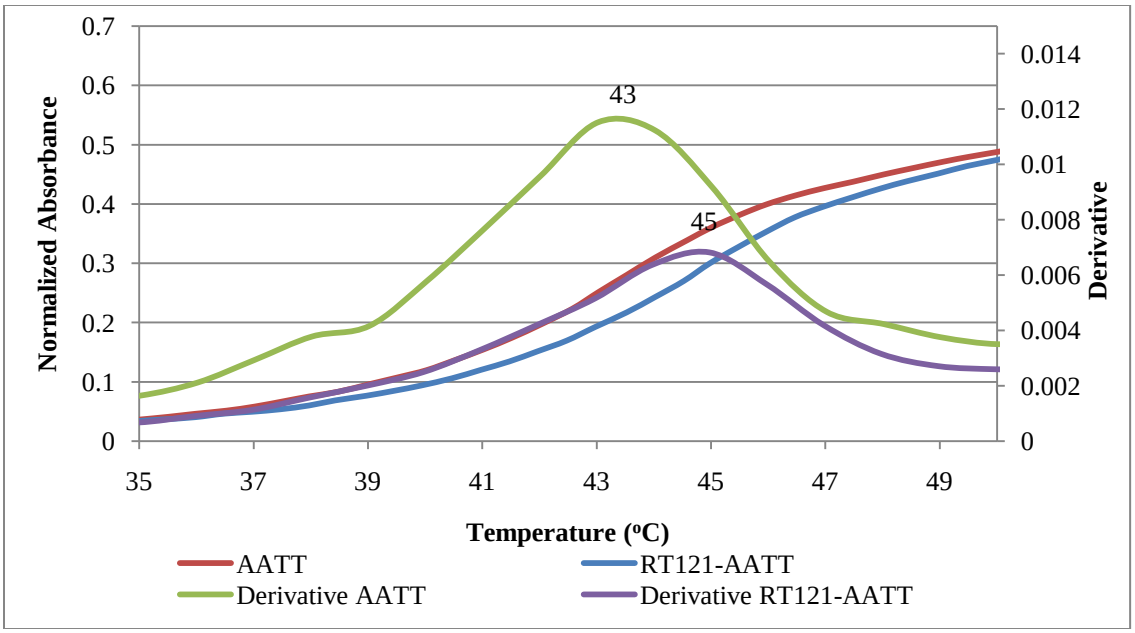

Figure 3.1 The effect of RT121 on the melting curve of AATT. The concentration of the compound to duplex DNA was 2:1 in CCl buffer. The normalized absorbance is on the primary axis on the left hand side of the plot. The first derivative is the secondary axis, which is plotted on the right hand side.

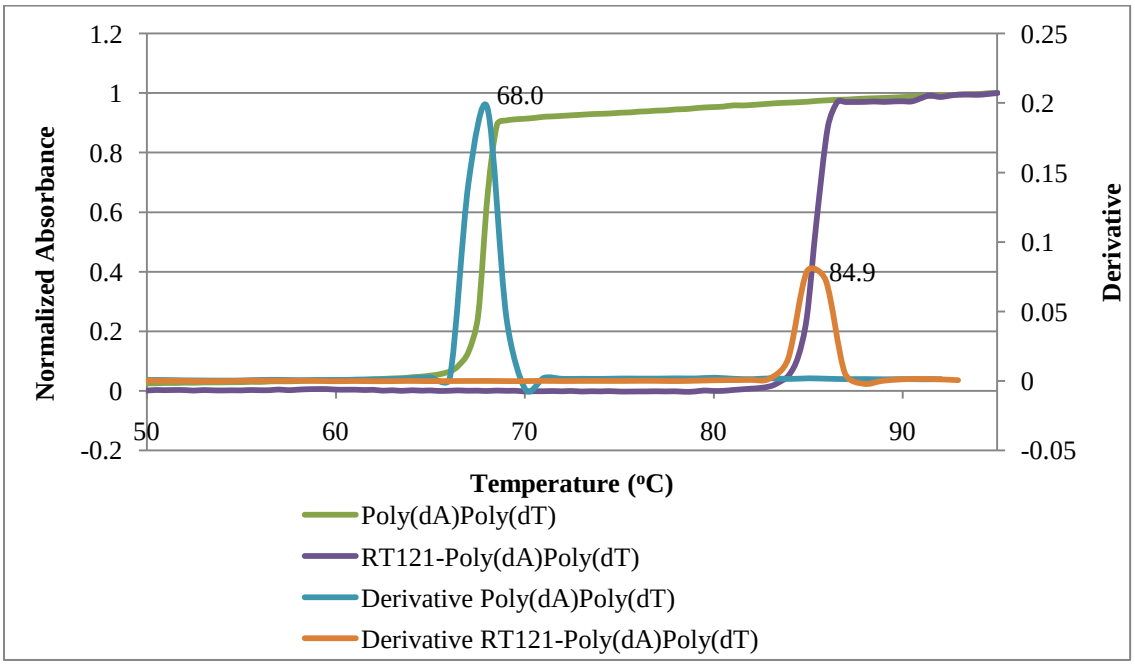

Figure 3.2 The effect of RT121 on the melting curve of Poly(dA)•Poly(dT). The concentration of the compound to polymer base pair was 1:1 in CCl buffer. The normalized absorbance is on the primary axis on the left hand side of the plot. The first derivative is the secondary axis which is plotted on the right hand side.

3.3 Isothermal Titration Calorimetry

ITC was used to monitor the absorbance or the release of heat upon binding of various compounds to AATT and ATAT DNA oligomers. The ITC curves were fitted using the Origin 7.0 software implementing a single binding site model with the binding constant, stoichiometry and change in enthalpy as fitting parameters. Upon injection of the ligand into the DNA oligomer AATT, most of the compounds had an exothermic reaction at 25 ^{o}C; the data is shown in Figure 3.3 and summarized in Table 3.4. However, RT121 did not produce any significant heat under the reaction conditions; therefore no binding data could be collected at this temperature. The lack of any significant heat was not due to aggregation effects for RT121, as the extinction coefficient calculation was determined up to a concentration of 165 μM. Since RT121 did not produce any significant heat at 25 ^{o}C, additional ITC experiments were performed at 40 ^{o}C and a binding constant for RT121 was determined to be 3.14 x 10^{5} M^{-1}; the data is shown in Figure 3.5 and summarized in Table 3.6. Upon comparison of the thermodynamic values for DNA binding of compounds at different temperatures, the $-T\Delta S$ value has a larger contribution to the ΔG at 25 ^{o}C; however at 40 ^{o}C, the ΔH has the larger contribution to ΔG, as shown in Figures 3.6 and 3.8.

Upon injection of the ligand into the DNA oligomer ATAT, all of the compounds had an exothermic reaction at 25 ^{o}C (Figure 3.4 and Table 3.5). Upon comparison of the thermodynamic values for compound binding to AATT and ATAT at 25 ^{o}C, the overall ΔG values are slightly larger for AATT, than for ATAT binding. The relative contributions of ΔH and $-T\Delta S$ vary among the different ligand-DNA combinations. The binding stoichiometry for all compounds to both AATT and ATAT was determined to be 1:1 by fitting.

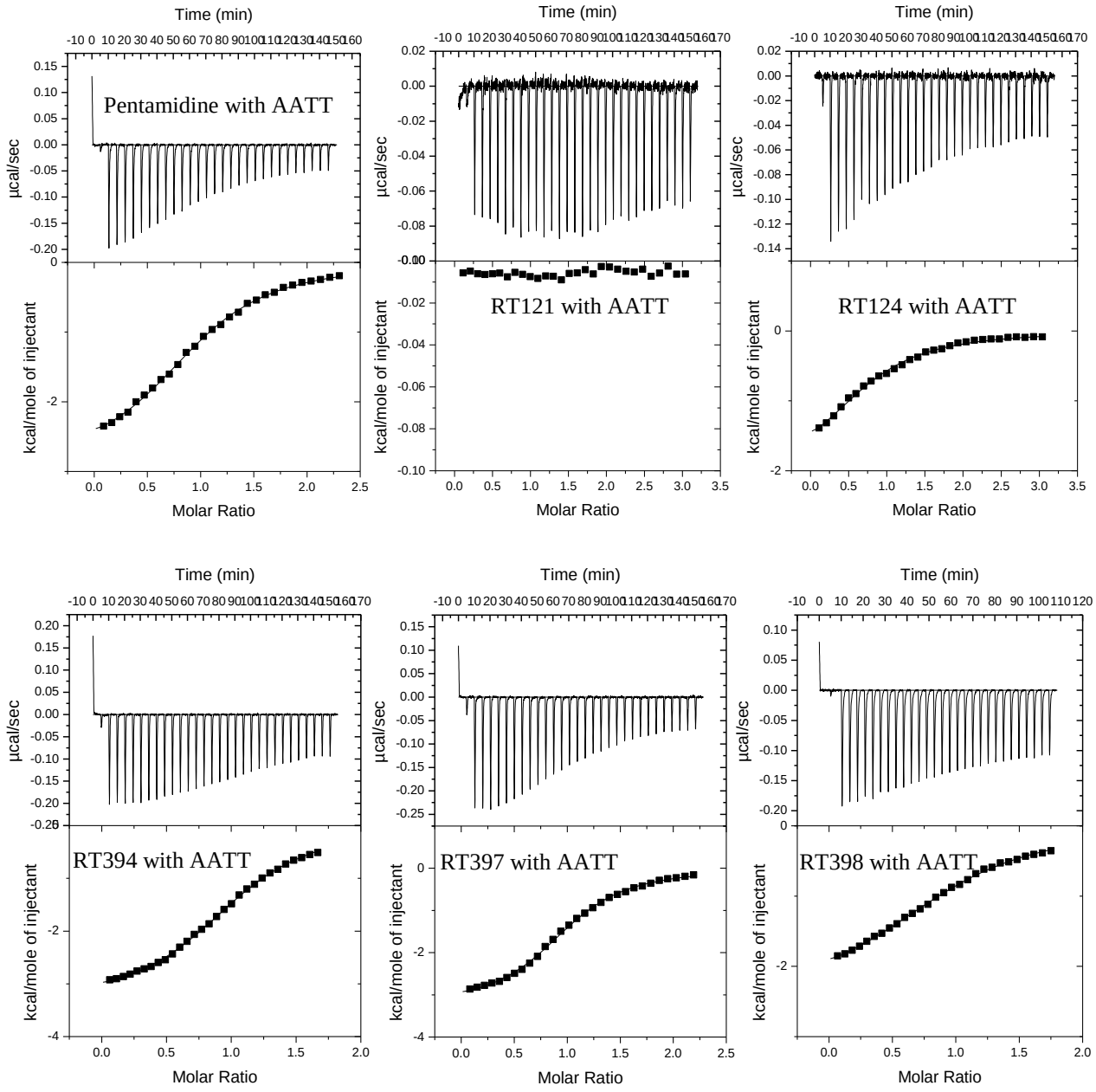

Figure 3.3 Calorimetry data for the titration of pentamidine analogs and AATT. Injections of 10 µL aliquots of 200 µM ligand into 20 µM AATT at 25 ^{o}C in CCl buffer. The ITC raw data, located in the top panel, is the power output per injection as a function of time. The bottom panel is the peak integration of the data that shows the heat produced per injection as a function of the duplex/ligand molar ratio.

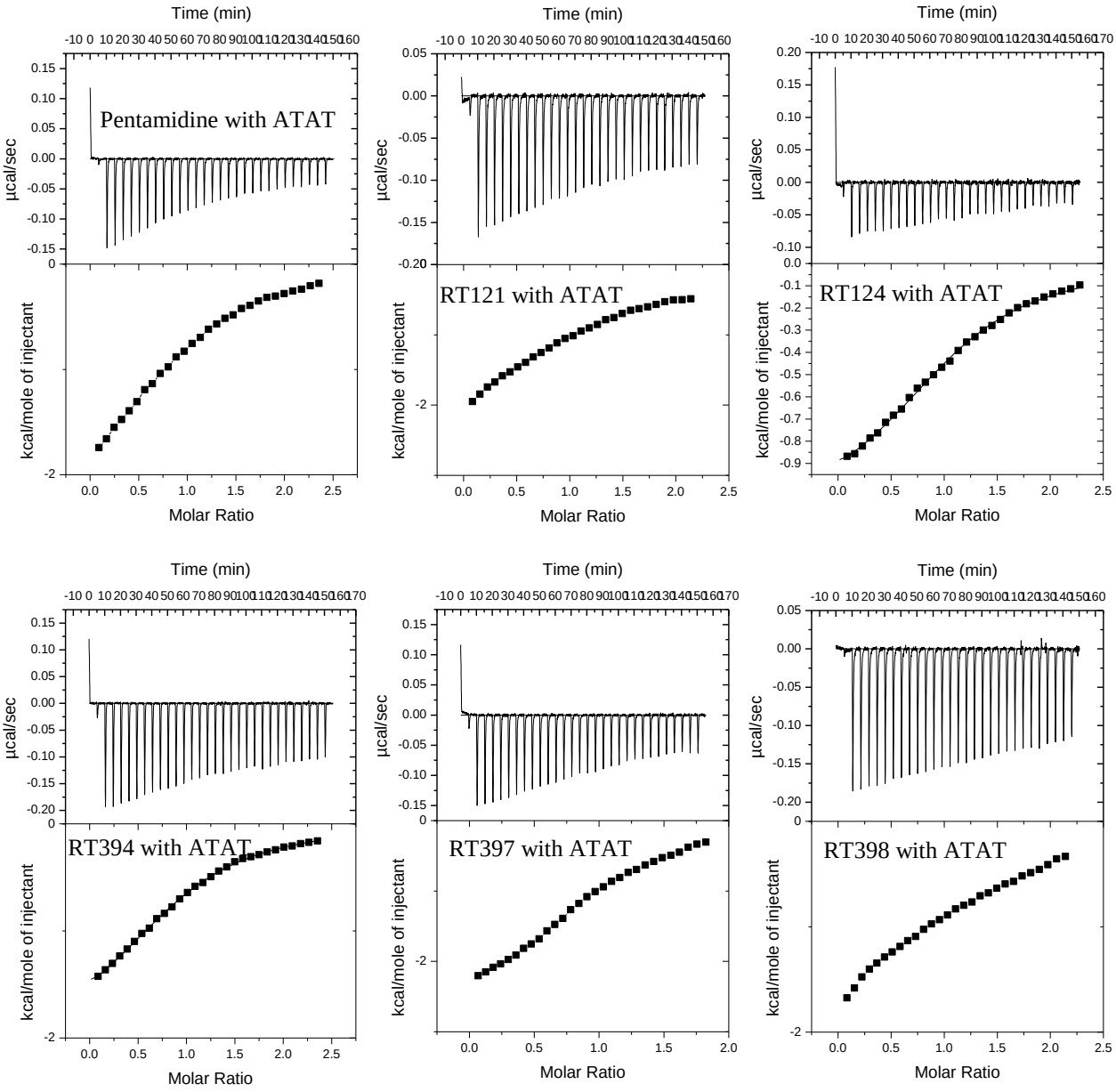

Figure 3.4 Calorimetry data for the titration of pentamidine analogs and ATAT. Injections of 10 µL aliquots of 200 µM ligand into 20 µM ATAT at 25 ^{o}C in CCl buffer. The ITC raw data, located in the top panel, is the power output per injection as a function of time. The bottom panel is the peak integration of the data that shows the heat produced per injection as a function of the duplex/ligand molar ratio.

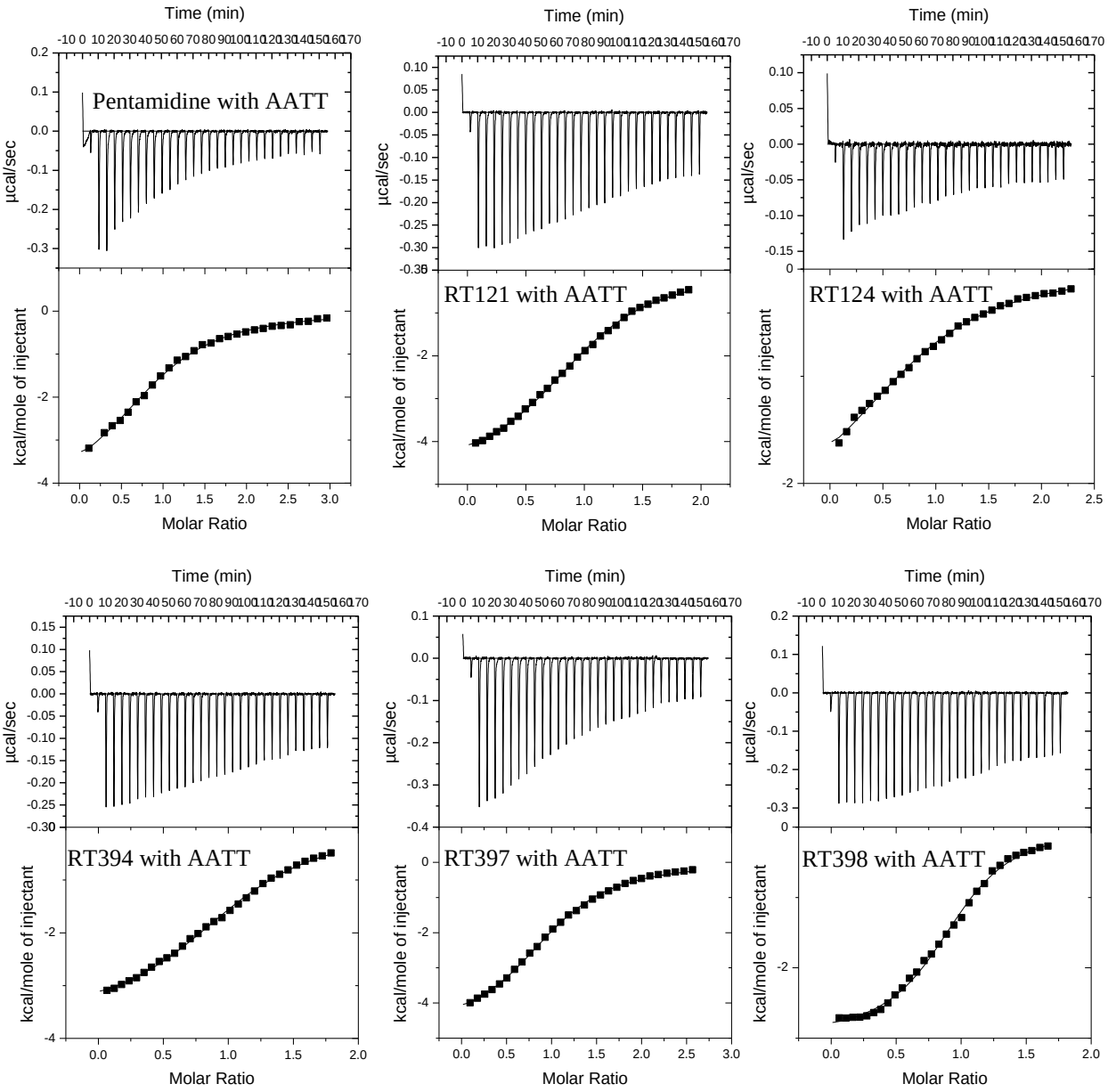

Figure 3.5 Calorimetry data for the titration of pentamidine analogs and AATT. Injections of 10 µL aliquots of 200 µM ligand into 20 µM AATT at 40 ^{o}C in CCl buffer. The ITC raw data, located in the top panel, is the power output per injection as a function of time. The bottom panel is the peak integration of the data that shows the heat produced per injection as a function of the duplex/ligand molar ratio.

Table 3.4 Thermodynamic values for pentamidine analogs and AATT at 25 °C in CCl buffer.

Ligand	Stoichiometry	K(10^5 M^{-1})	ΔH (cal/mol)	-TΔS (cal/mol)	ΔG (cal/mol)
Pentamidine	0.98 ± 0.05	2.5 ± 0.2	-2890 ± 60	-4500 ± 100	-7400
RT121	No data available				
RT124	1 ± 0.2	0.89 ± 0.2	-1690 ± 70	-5070 ± 40	-6800
RT394	1.03 ± 0.02	4.4 ± 0.6	-3320 ± 20	-4380 ± 90	-7700
RT397	1.04 ± 0.04	4.2 ± 0.2	-3190 ± 90	-4470 ± 30	-7700
RT398	0.96 ± 0.03	1.7 ± 0.6	-2470 ± 60	-4680 ± 60	-7100

Table 3.5 Thermodynamic values for pentamidine analogs and ATAT at 25 °C in CCl buffer.

Ligand	Stoichiometry	K(10^5 M^{-1})	ΔH (cal/mol)	-TΔS (cal/mol)	ΔG (cal/mol)
Pentamidine	0.98 ± 0.07	1.26 ± 0.04	-2800 ± 200	-4200 ± 200	-7000
RT121	1.10 ± 0.08	0.559 ± 0.009	-3500 ± 200	-3000 ± 100	-6500
RT124	1.1 ± 0.1	1.6 ± 0.1	-1140 ± 60	-6000 ± 100	-7100
RT394	0.96 ± 0.03	1.2 ± 0.1	-2300 ± 400	-4800 ± 300	-6900
RT397	0.94 ± 0.03	2.14 ± 0.02	-2760 ± 40	-4500 ± 30	-7300
RT398	1.00 ± 0.01	0.515 ± 0.008	-3420 ± 40	-3000 ± 20	-6400

Table 3.6 Thermodynamic values for pentamidine analogs and AATT at 40 °C in CCl buffer.

Ligand	Stoichiometry	K(10^5 M^{-1})	ΔH (cal/mol)	-TΔS (cal/mol)	ΔG (cal/mol)
Pentamidine*	0.95	1.8	- 4200	-3200	-7500
RT121	1.01 ± 0.02	3.1 ± 0.2	-5200 ± 700	-2400 ± 600	-7900
RT124	1.0 ± 0.2	1.1 ± 0.2	-2400 ± 30	-4800 ± 100	-7200
RT394	1.09 ± 0.01	2.5 ± 0.5	-3900 ± 400	-3600 ± 600	-7700
RT397	0.99 ± 0.04	2.04 ± 0.7	-5400 ± 700	-2000 ± 900	-7600
RT398	0.98 ± 0.03	6.08 ± 0.7	-3300 ± 300	-4800 ± 300	-8300

* Only one trial was performed with pentamidine

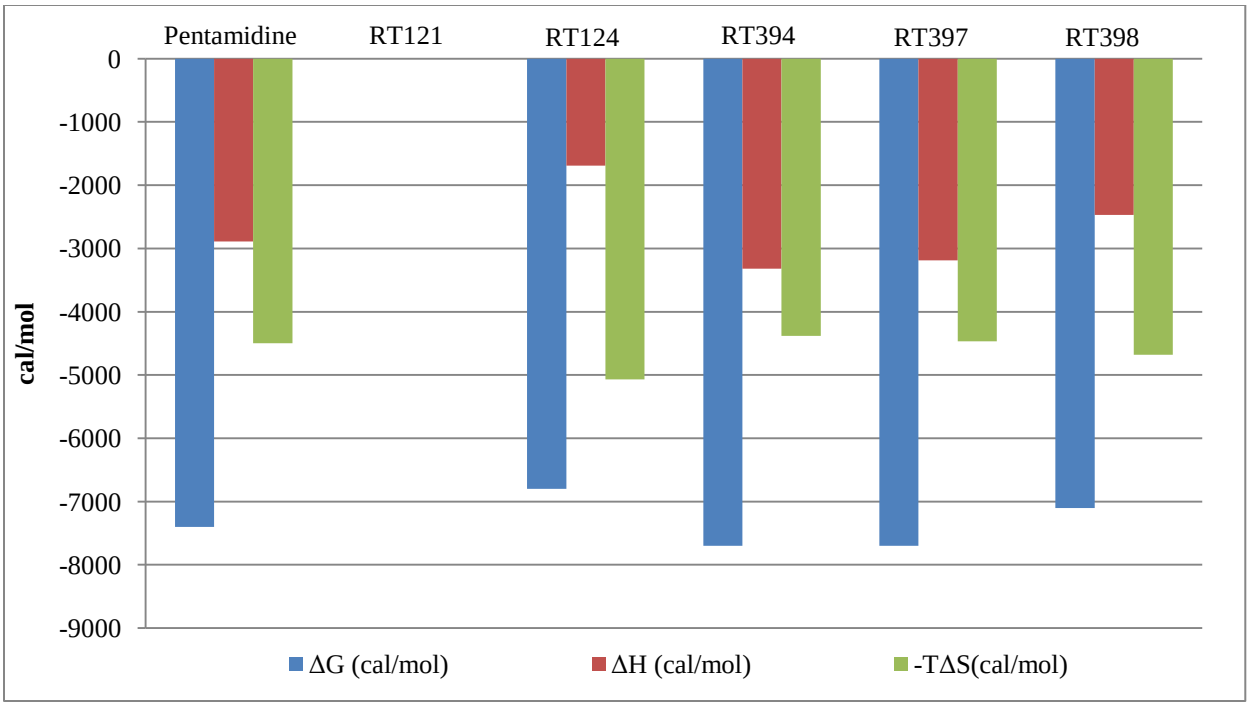

Figure 3.6 Comparison of thermodynamic values of pentamidine analogs with AATT at 25 ^{o}C.

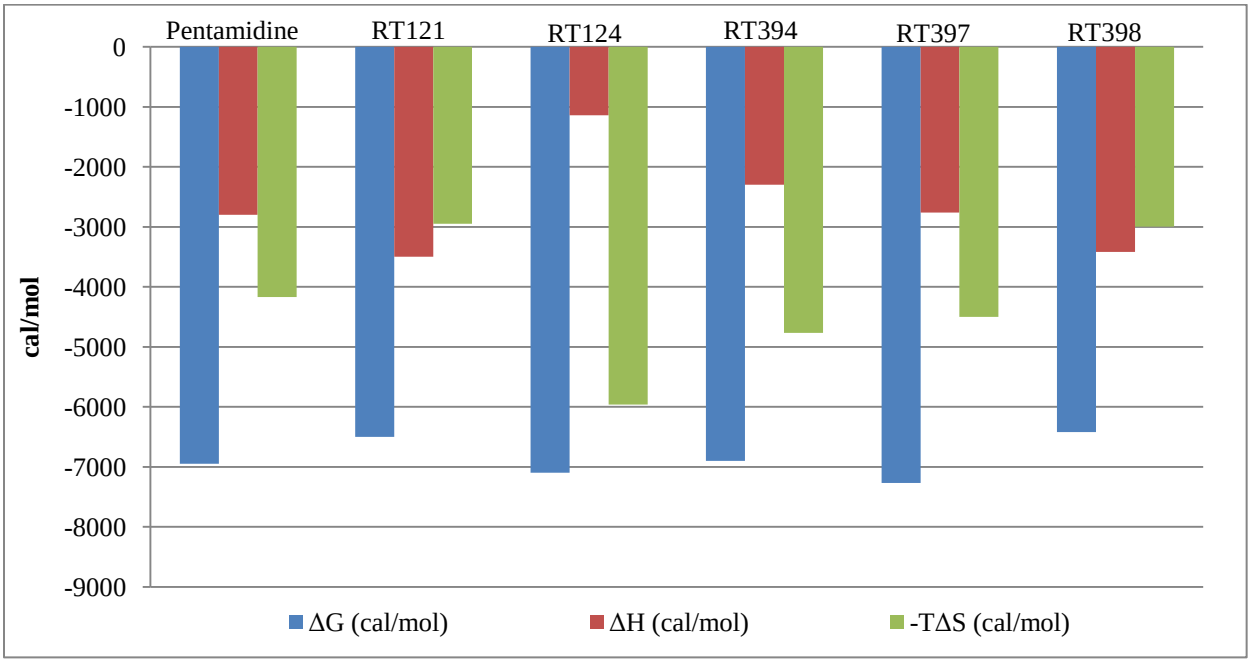

Figure 3.7 Comparison of thermodynamic values of pentamidine analogs with ATAT at 25 ^{o}C.

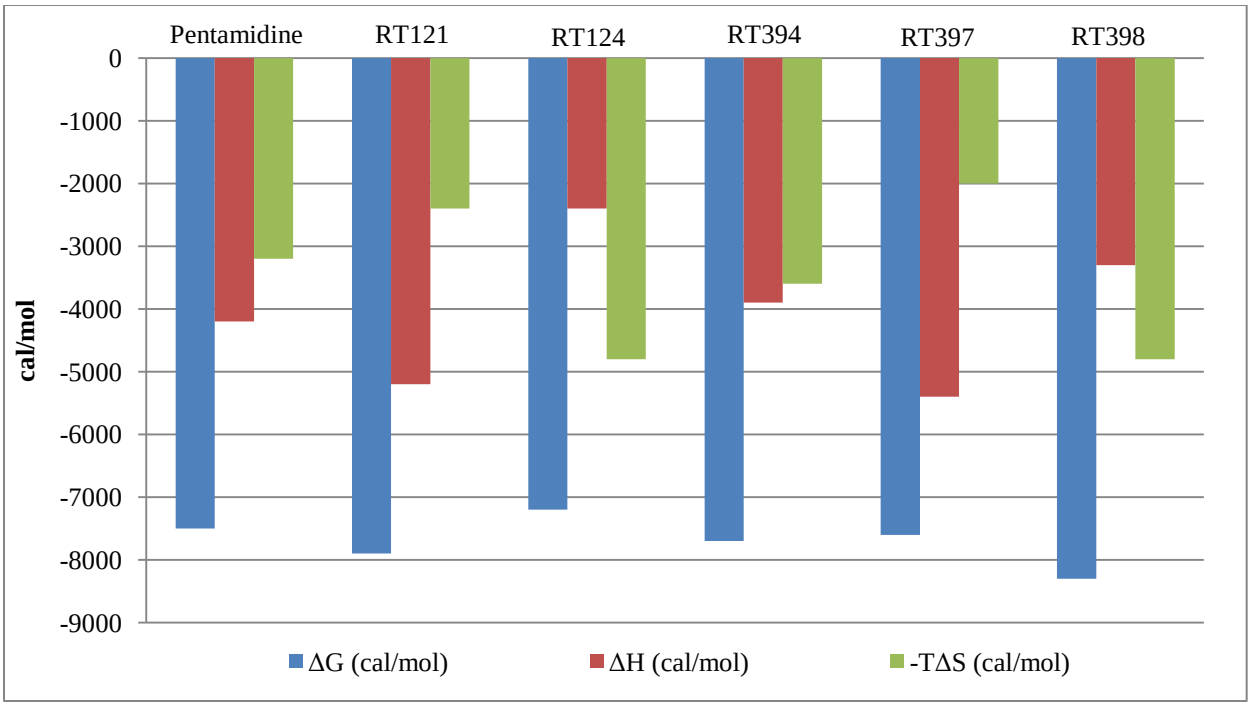

Figure 3.8 Comparison of thermodynamic values of pentamidine analogs with AATT at 40 ^{o}C.

3.4 Fluorescence

The fluorescence titrations, shown in Figures 3.9 and 3.10 and summarized in Table 3.7, were corrected for dilution and normalized. The fluorescence titration data were fitted using Origin 7.0 software for one binding site using enhancement factor and binding constant as fitting parameters, see equations in section 2.7. The fluorescence for RT121, RT394, RT397 and RT398 increased upon the addition of DNA. Upon comparison with the ITC results for RT394, RT397 and RT398 with AATT at 25^{o}C, the general trend for the binding constant was similar. RT394 and RT397 have nearly the same binding constant values, which are several times larger than the binding constant for RT398.

Both pentamidine and RT124 initially showed a low fluorescence intensity. Upon addition of DNA, an additional decrease in fluorescence intensity was observed as can be seen in Figure 3.9. The low fluorescence intensity for these two compounds combined and thus the low signal to noise ratio of the data made it difficult to obtain an accurate enhancement factor. The data for these two compounds was fit to determine an approximate binding constant using several different possible enhancement factors under 1; an approximate value for a binding constant for both compounds was 10^5 M^{-1}

Table 3.7 Binding data for fluorescence titrations of pentamidine analogs with AATT at 25 ^{o}C in CCl buffer.

Ligand	Enhancement Factor	K (10^5 M^{-1})	ΔG (cal/mol)
Pentamidine	Less than 1	Approximately 10^5 M^{-1}	Approximately -7000
RT121	9.6 ± 0.1	3.7 ± 0.2	-7600
RT124	Less than 1	Approximately 10^5 M^{-1}	Approximately -7000
RT394	8.1 ± 0.1	0.92 ± 0.05	-6800
RT397	13.3 ± 0.4	1.0 ± 0.1	-6800
RT398	7.5 ± 0.1	0.26 ± 0.01	-6000

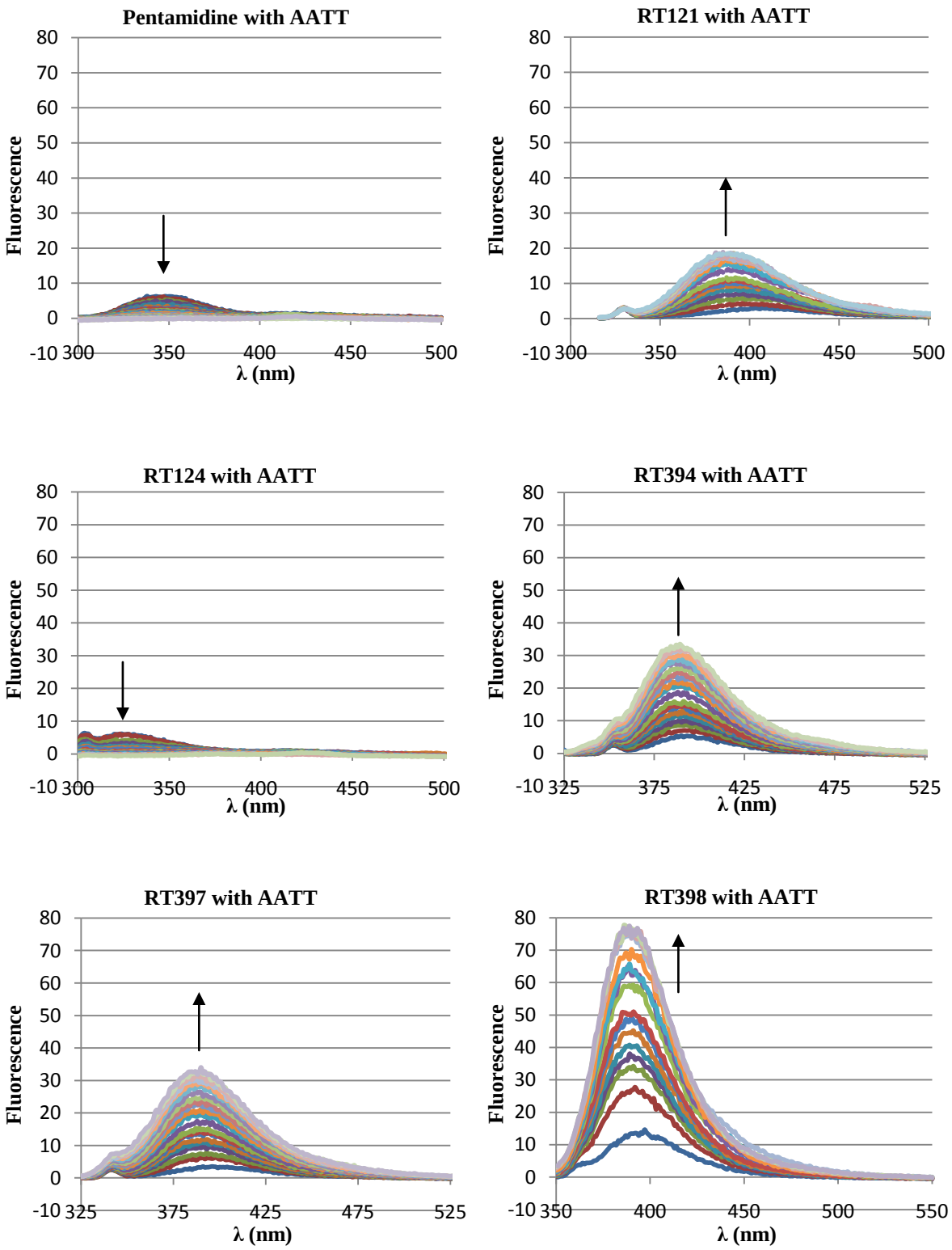

Figure 3.9 Fluorescence by wavelength for titrations of 0.5 µM pentamidine analogs with AATT at 25 °C in CCl buffer. The arrows indicate the change in fluorescence upon addition of DNA.

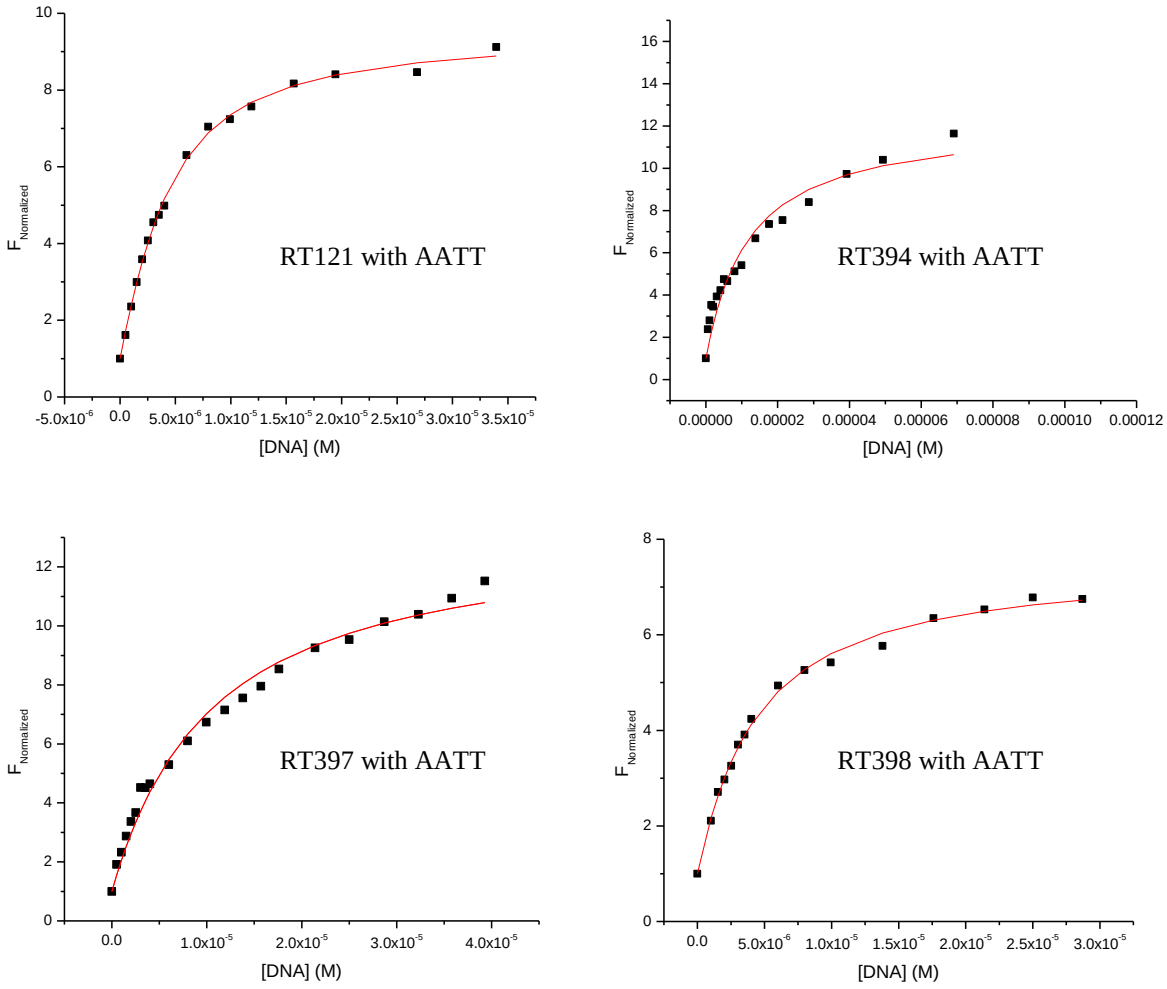

Figure 3.10 Fluorescence binding isotherms for pentamidine analogs and AATT at 25 ^{o}C in CCl buffer.

3.5 Error Analysis of Binding Constant and Thermodynamic Values

The error presented in Tables 3.4, 3.5 and 3.7, which is generally below 15%, is based on the reproducibility of the results. Additionally, the ITC data was fit using Origin 7.0 using a single site binding model, which determines an error in the actual fitting of the individual curve from the values for the binding constant, stoichiometry and change in enthalpy. The actual error for fitting of the curve was generally below 10%. Both of these error values are reasonable for this technique.

All of the compounds in this study are considered to be weak binding compounds, which complicates the actual fitting of the data. The fitting is performed after the baseline is adjusted for instrument noise; however, with a weak binding compound the adjustments in the baseline can cause a significant impact on reproducibility. The weaker binding observed with the ATAT oligomer did generate an increase in fitting error compared to the AATT oligomer. Additional complications exist for the determination of ΔH, and consequently ΔS; upon integration of the data, there are incremental changes in ΔH with each injection, therefore the actual value for ΔH is extrapolated, which can be inaccurate. However, under the experimental conditions the binding constant for these compounds is more reliable.

4 Discussion

4.1 Extinction Coefficient and Fluorescence Intensity

The titrations, with data in Table 3.1, show that the absorbance maxima for the pentamidine analogs are shifted to a higher wavelength, which may be advantageous for other spectroscopic techniques, since DNA has a maximum wavelength at 260 nm. This bathochromic shift is due to the presence of the nitrogen and sulfur atoms in the linker region. The extinction coefficient is a property of the molecule undergoing an electronic transition; generally these are the bonding electrons. The larger the extinction coefficient is due to the greater probability that the electronic transition will take place; 10^3 M^{-1} cm^{-1} is considered low-intensity absorption and 10^6 M^{-1} cm^{-1} is considered high-intensity absorption[17]. The extinction coefficients for the pentamidine analogs are all higher than pentamidine, except for RT124, which is significantly less. This shift to higher wavelength and increase in extinction coefficient is also seen in DB75, with a maximum wavelength at 360 nm and an extinction coefficient of 36,600 M^{-1} cm^{-1}.[32]

Fluorescence intensity depends directly on the concentration of the fluorophore, extinction coefficient and quantum yield. The probability that a fluorophore will emit a photon is a product of the probability that a photon is absorbed and the probability that an excited state decays by emitting a photon, which is related to quantum yield. The probability of absorption is expressed by the extinction coefficient.[33] Comparing the fluorescence intensities to the extinction coefficient, which is only one factor, it can be seen that the sulfur and nitrogen analogs show the same trend in fluorescence intensity as the extinction coefficients. The analog with the highest extinction coefficient has the most fluorescence intensity. The order from highest to

lowest is RT398 > RT394 ≈ RT397 > RT121. Additionally, RT121, RT394, RT397 and RT398 had an increase in fluorescence intensity upon binding to duplex AATT DNA. In a recent study, a propamidine analog with a nitrogen linker also showed a large increase in fluorescence intensity upon sequence-specific AT duplex DNA binding.[34] Both of the compounds that contained oxygen, pentamidine and RT124, both show a decrease in fluorescence intensity upon binding to DNA. The increased fluorescence intensity of the RT121, RT394, RT397 and RT398 upon binding to AATT are positive results, since this will enable additional fluorescence studies, such as fluorescence microscopy, to be performed, which will help determine where these compounds accumulate in the cell.

4.2 Thermal Melting

Several different DNA with varied A/T site length were investigated to determine any possible trends for binding affinity by the change in melting temperature. The investigated compounds all showed similar ΔT_m values for the AATT oligomer indicating a similar binding constant to this DNA sequence (See data located in Table 3.3). For the A_3T_3 sequence, the RT394, RT397, and RT398 ΔT_m values were slightly higher than with pentamidine, suggesting that the nitrogen linker has slightly improved the binding affinity, thereby increasing the thermal stability of the DNA. However, the AAAA oligomer with pentamidine has ΔT_m of 1 ^oC, where RT394, RT397 and RT398 had a ΔT_m of 0 ^oC. This suggests that the nitrogen linked compounds may not bind at all to this oligomer. Interestingly, when the oligomer is Poly(dA)•Poly(dT), the RT394, RT397 and RT398 do indeed bind. This suggests that these compounds need more than 4 A bases in a row to bind, when there are no A bases on the opposite strand. The Poly(dA)•Poly(dT) showed the largest ΔT_m with RT121. Since the sulfur has a slightly larger radius than oxygen, perhaps it has improved hydrogen bonding with the O4' of the deoxyribose

backbone than with pentamidine. The lowest ΔT_m for the Poly(dA)•Poly(dT) was with RT124, possibly due to steric hindrance upon binding of the sulfonyl group in the narrow minor groove of the Poly(dA)•Poly(dT) oligomer. RT394, RT397 and RT398 with Poly(dA)•Poly(dT) had similar ΔT_m values, indicating no preference for any of the terminal amidinium substitutions over the RT394.

4.3 Binding Constants and Thermodynamics

The ITC curves, in Figure 3.3 and summarized in Table 3.4, show that pentamidine and RT compounds bind to AATT at 25 ^oC with slightly different affinity, which is consistent with the similar ΔT_m values. The pentamidine binding constant was determined to be 2.5 (± 0.2) x 10^5 M^{-1}. The literature value for pentamidine with 5'-CGC GCA ATT GCG CG-3' at 25 ^oC is 1.8 (± 0.3) x 10^6 M^{-1}; in addition to the DNA being one base pair longer, the salt concentration was 50 mM NaCl, which can account for some of the discrepancy in binding constants.[31] The buffer used in this research contained 100 mM NaCl; due to the lower salt concentration in the buffer the electrostatic interactions between the positively charged ligand and the negatively charged DNA are generally increased and the binding constant is expected to be higher.[35] To verify the impact of the NaCl concentration on the binding constant for pentamidine, the following equation was used:

where K_{obs} is the observed binding constant at the particular conditions, K is the binding constant, m is the number of phosphates that interact with the compound (generally, the charge of the compound, in this case m = 2), and M^+ is the concentration of Na^+ ions in the buffer.[6] The changes in NaCl concentration account for approximately 65% of the error in the experimental

and literature value for the pentamidine binding constant. The RT394 and RT397 bind with slightly higher affinity than pentamidine to AATT at 25 ^{o}C, since the binding constants are both approximately 4 x 10^{5} M^{-1}. This suggests that changing the linker to nitrogen is a promising way to improve binding. Thus, confirming the predicted higher binding affinity for the unsubstituted nitrogen linked RT394 as described in the1993 molecular modeling study performed by Greenidge, et al.[16] Furthermore, this similarity in binding affinity suggests that the isopropyl substitution on RT397 does not have a negative effect on binding. As previously stated, the amidinium groups of pentamidine hydrogen bond to the DNA in the minor groove, the nitrogen analogs RT397 and RT398 may bind in the same manner. Therefore, since RT397 and RT398 have nearly the same binding constant, this indicates that the isopropyl group of RT397 is most likely pointed out of the minor groove. The binding constant for RT398 was determined to be 1.7 x 10^{5} M^{-1}, which is similar to pentamidine, but less than the other nitrogen analogs. Since the RT398 has the nitrogen substitution in the linker, it should have improved binding over pentamidine. However it is slightly reduced, which is likely due to the less flexible nature of the imidazoline ring of RT398. The binding constant for RT124 was less than all the other compounds at a value of 8.9 (± 2) x 10^{4} M^{-1}. As described above, this might be caused by a steric hindrance of the sulfonyl group in the minor groove. Additionally, as seen in previous studies, the bond angle between the sulfonyl and the benzene rings has been seen at a nearly 90^{o} angle, which would prevent the compound from properly fitting the shape of the minor groove.[36]

The fluorescence titration results augment the ITC values, located in Figure 3.10 and summarized in Table 3.7. The actual values for the binding constants are in good agreement with the values calculated for ITC, with the regards to the increased concentrations used to determine the binding constants. For pentamidine and RT124, the fluorescence was decreased,

while it was increased for RT121, RT394, RT397, and RT398, as seen in Figure 3.9. Since, the fluorescence for pentamidine and RT124 were very low, less than 10 fluorescence units, therefore the actual fluorescence enhancement factor was difficult to calculate. However, fitting was attempted, for both of these compounds, for a range of enhancement factor from 2×10^{-1} to 2×10^{-5} which consistently produced a binding constant with the same order of magnitude at 10^5 M^{-1}. The trends for RT394, RT397 and RT398 were the same as in ITC. RT394 and RT397 had similar binding constants of approximately 1×10^5 M^{-1}. The binding constant for RT398 was less than RT394 and RT397, with a value of 2.6×10^4 M^{-1}. The RT121, which did not have any data for the ITC, did show binding close to that of pentamidine, indicating that the binding is entropically driven.

Using the ITC data, the ΔG was calculated from equation 1.2. The ΔG for RT121 was not able to be calculated from ITC, since little heat was generated during the titration. The RT121 does in fact bind to AATT at 25 ^{o}C as shown by the fluorescence titration data, as described above. Therefore ΔG for RT121 is based on fluorescence data, unlike the other analogs. All of the compounds had a negative ΔG which shows that the reactions were all spontaneous at 25 ^{o}C with AATT. All of the compounds, with the exception of RT121, showed exothermic binding and thus a negative ΔH. All of the compounds showed a positive ΔS upon binding and thus highlight the importance of entropic contributions. The negative ΔH can be explained by the formation of hydrogen bonds, van der Waals contacts and electrostatic interactions between the ligand and the DNA. Additionally, the ΔH will also account for the unfavorable loss of hydrogen bonds between DNA and solvent, or salt and DNA interactions. The positive ΔS can partly be accounted for by the free compound going from the bulk solvent where water molecules are in a more ordered state to avoid contact with the hydrophobic ligand

to a bound state which releases this water back into the less ordered bulk solvent, as well as releasing ordered water molecules from the minor groove.[9]

The comparison of the contributions of the enthalpy and entropy to the Gibbs' free energy shows that at 25 ^{o}C all of the binding reactions with AATT were driven by the entropic contribution; especially RT121 and RT124 which had nearly 100% and 75%, respectively, of the value of ΔG contributed by the entropy. Similarly, DB75 is significantly driven by entropy at 25 ^{o}C, approximately 80%.[37] Pentamidine and RT398 had relatively similar entropic contributions of -4500 (± 100) and -4680 (± 60) cal/mol, respectively. However, pentamidine had a larger contribution from enthalpy, as compared to RT398. The RT398 had the largest contribution to entropy of all the nitrogen analogs. This can be contributed, in part, to the imidazoline ring system having less unfavorable entropy loss, since it has fewer degrees of freedom as a free ligand. Similarly, DB75 has less unfavorable entropy loss, due to its rigidity.[37] The ΔG for RT394 and RT397 were both -7700 cal/mol, with approximately the same values for ΔH and –TΔS. This similar distribution of the Gibbs' free energy for RT394 and RT397 further suggests that they bind in a similar manner, as described above.

The ITC curves show that pentamidine and RT compounds generally bind to ATAT at 25 ^{o}C with lower affinity than with AATT, located in Figure 3.4 and summarized in Table 3.5. The lower binding affinity can possibly be attributed to the fact that the binding site is slightly wider for ATAT than with the AATT site, 4.6 Å and 3.8 Å respectively.[38] The wider binding site in ATAT would decrease the ability for the compounds to be able to hydrogen bond and decrease the van der Waals contacts without bigger structural changes to the DNA. The decrease in ΔH for most of these compounds indicates that these types of interactions were likely reduced. However, the wider groove of ATAT appears to have improved the binding for the bulky

sulfonyl group linker of RT124. There is a decreased electrostatic potential for the wider ATAT minor groove, which might additionally account for the lower binding affinity for the analogs with ATAT.[38] Due to the increased ordered hydration of the AATT minor groove over ATAT, as suggested by the crystal structures, one would expect the entropy contribution for binding to ATAT to be less than AATT, however this was not observed for all of the analogs.[39,40] Only the pentamidine, RT398, and likely the RT121 had the decrease in entropy, as expected. The difficultly in the extrapolation of ΔH and consequently the calculation of ΔS, as previous described in the error analysis, may possibly explain this discrepancy. However it should be noted that under the experimental conditions, the calculation of the binding constant is more reliable.

The ITC curves, in Figure 3.5 and summarized in Table 3.7, show that the all the compounds bind to AATT at 40^{o}C with slightly different affinity and binding constants as compared to 25 ^{o}C. However, the ΔG was nearly constant with the increase in temperature from 25 ^{o}C to 40 ^{o}C for pentamidine, RT394 and RT397. Interestingly, this result has been seen previously with the minor groove binding analogs of DB75, which is also a pentamidine analog.[37] Similarly a nearly constant ΔG is seen for common processes, such as protein folding and protein-DNA interactions, that have a major hydrophobic component in their Gibbs' free energy.[41,42,43] Since the free energy changed very little for these analogs, there is significant compensation in the balance of enthalpy and entropy contributions and the ΔH actual becomes the driving force at 40 ^{o}C, whereas at 25 ^{o}C the driving force is the entropy. Unlike the other compounds, RT124 and RT398 did not maintain a constant ΔG over the two temperatures; they both had an increase in ΔG. Furthermore, the driving force of RT124 and RT398 continued to be driven entropically. Comparing the ΔH values at 25 ^{o}C to the values at 40 ^{o}C show that all of

the compounds have a negative heat capacity, assuming ΔH for RT121 is nearly zero at 25 ^{o}C. The negative heat capacities indicate that hydrophobic effects play a significant role on binding of the compounds, as seen in previous studies with DB75 and Hoeschst 33258.[37,9]

Comparing the binding and thermodynamic data to the biological data, previously mentioned in the introduction, does not appear to have any specific correlation. The analogs all were active in vitro, however, RT121 and RT397 were not active in vivo.[15] This is most likely due to reasons other than thermodynamics, such as the inability to reach the DNA target. Specifically citing RT397 as compared to RT394, which was active in vivo, had very similar ΔT_m, binding constants, as well as relative contributions to free energy by enthalpy and entropy. Additional the RT398, generally had a lower Gibbs' free energy as compared to the other compounds in this study, yet it had the highest selectivity in vitro, as well as the highest cure rate of 4 out of 4 for mice infected with trypanosomiasis, further suggesting that there is no simple correlation between ligand-DNA thermodynamics and the biological activity.[15]

5 Conclusion

All of the pentamidine analogs interacted with the investigated AT rich DNA sequences. All of the analogs, except for RT124, had a significant increase in fluorescence upon binding to DNA, which will enable future work to be done with fluorescence microscopy to help determine if and where these compounds accumulate in the target organism, such as the trypanosome. The nitrogen substitution in the linker of pentamidine provides a slight increase of the binding affinity with AT rich DNA, possibly due to increased van der Waals contacts in the minor groove. The substitution of the terminal amidinium group with an isopropyl group does not appear to affect the binding affinity significantly; however a less flexible imidazoline

substitution counteracts the improved binding affinity from the nitrogen linker. The general driving force of the binding with the investigated DNA sequences at 25 ^{o}C is the entropy. However, the opposite is generally true at 40 ^{o}C, where the binding reaction is driven by the enthalpy. Both of these suggest that hydrophobic interactions play a major role for the binding event. The binding affinity is generally decreased when the DNA is changed from non-alternating AT to an alternating AT site. A simple correlation between ligand-DNA thermodynamics and the biological activity was not able to be determined.

This binding study provides new information on the thermodynamic values for these compounds binding with AT rich DNA. Additionally, this provides more information to determine any general patterns for thermodynamic values to aid in future drug design.

6 References

1. Garbett, N.; Chaires, J. B., Binding: A Polemic and Rough Guide. *Methods in Cell Biology* **2008,** *84*, 3-21.

2. Engel, T.; Reid, P., *Thermodynamics, statistical thermodynamics, and kinetics*. Pearson Benjamin Cummings: San Francisco, 2006; p xiv, 589 p.

3. Blumenfeld, L. A.; Tikhonov, A. N., *Biophysical thermodynamics of intracellular processes : molecular machines of the living cell*. Springer-Verlag: New York, 1994; p viii, 177 p.

4. Haq, I.; Chowdhry, B. Z.; Jenkins, T. C., Calorimetric techniques in the study of high-order DNA-drug interactions. *Methods Enzymol* **2001,** *340*, 109-49.

5. Haynie, D. T., *Biological thermodynamics*. Cambridge University Press: Cambridge ; New York, 2001; p xv, 379 p.

6. Van Holde, K. E.; Johnson, W. C.; Ho, P. S., *Principles of physical biochemistry*. 2nd ed.; Pearson/Prentice Hall: Upper Saddle River, N.J., 2006; p xiii, 710, 27 p.

7. Neidle, S., *Principles of nucleic acid structure*. 1st ed.; Academic Press: Amsterdam, 2008; p xii, 289 p.

8. Blackburn, G. M., *Nucleic acids in chemistry and biology*. 3rd ed.; RSC Pub.: Cambridge, UK, 2006; p xxxi, 470 p.

9. Haq, I., Thermodynamics of drug-DNA interactions. *Arch Biochem Biophys* **2002,** *403* (1), 1-15.

10. Wilson, W. D.; Tanious, F. A.; Mathis, A.; Tevis, D.; Hall, J. E.; Boykin, D. W., Antiparasitic compounds that target DNA. *Biochimie* **2008,** *90* (7), 999-1014.

11. Demeunynck, M.; Bailly, C.; Wilson, W. D. E., *Small Molecule DNA and RNA Binders*. Wiley-VCH: 2003; Vol. 2, p 732.

12. Paine, M. F.; Wang, M. Z.; Generaux, C. N.; Boykin, D. W.; Wilson, W. D.; De Koning, H. P.; Olson, C. A.; Pohlig, G.; Burri, C.; Brun, R.; Murilla, G. A.; Thuita, J. K.; Barrett, M. P.; Tidwell, R. R., Diamidines for human African trypanosomiasis. *Curr Opin Investig Drugs* **2010,** *11* (8), 876-83.

13. Fairlamb, A. H., Chemotherapy of human African trypanosomiasis: current and future prospects. *Trends Parasitol* **2003,** *19* (11), 488-94.

14. Edwards, K. J.; Jenkins, T. C.; Neidle, S., Crystal structure of a pentamidine-oligonucleotide complex: implications for DNA-binding properties. *Biochemistry* **1992,** *31* (31), 7104-9.

15. Bakunova, S. M.; Bakunov, S. A.; Patrick, D. A.; Kumar, E. V.; Ohemeng, K. A.; Bridges, A. S.; Wenzler, T.; Barszcz, T.; Jones, S. K.; Werbovetz, K. A.; Brun, R.; Tidwell, R. R., Structure-activity study of pentamidine analogues as antiprotozoal agents. *J Med Chem* **2009,** *52* (7), 2016-35.

16. Greenidge, P. A.; Jenkins, T. C.; Neidle, S., DNA minor groove recognition properties of pentamidine and its analogs: a molecular modeling study. *Mol Pharmacol* **1993,** *43* (6), 982-8.

17. Pavia, D. L.; Lampman, G. M.; Kriz, G. S., *Introduction to spectroscopy : a guide for students of organic chemistry*. 3rd ed.; Harcourt College Publishers: Fort Worth, 2001; p xiv, 579, 15, 47, 8 p.

18. Wilson, W. D.; Tanious, F. A.; Fernandez-Saiz, M.; Rigl, C. T., Evaluation of Drug-Nucleic Acid Interactions by Thermal Melting Curves. *Methods in Molecular Biology* **1998,** *90*, 219-240.

19. Mathews, C. K.; Van Holde, K. E., *Biochemistry*. 2nd ed.; Benjamin/Cummings Pub. Co., Inc.: Menlo Park, Calif., 1996; p xxvii, 1159 p.

20. Schildkraut, C., Dependence of the melting temperature of DNA on salt concentration. *Biopolymers* **1965,** *3* (2), 195-208.

21. Hamaguchi, K.; Geiduschek, E. P., The Effect of Electrolytes on the Stability of the Deoxyribonucleate Helix. *Journal Of American Chemical Society* **1962,** *84* (8), 1329-1338.

22. Chaires, J. B., Calorimetry and thermodynamics in drug design. *Annu Rev Biophys* **2008,** *37*, 135-51.

23. Breslauer, K. J.; Freire, E.; Straume, M., Calorimetry: a tool for DNA and ligand-DNA studies. *Methods Enzymol* **1992,** *211*, 533-67.

24. Wiseman, T.; Williston, S.; Brandts, J. F.; Lin, L. N., Rapid measurement of binding constants and heats of binding using a new titration calorimeter. *Anal Biochem* **1989,** *179* (1), 131-7.

25. Ladbury, J. E., Calorimetry as a tool for understanding biomolecular interactions and an aid to drug design. *Biochem Soc Trans* **2010,** *38* (4), 888-93.

26. Picard, D., *Nuclear receptors : a practical approach*. Oxford University Press: New York, 1999; p xviii, 285 p.

27. Eftink, M. R., Fluorescence Methods for Studying Equilibrium Macromolecule-Ligand Interactions. *Methods in Enzymology* **1997,** *278*, 221-257.

28. Mathis, A. M.; Holman, J. L.; Sturk, L. M.; Ismail, M. A.; Boykin, D. W.; Tidwell, R. R.; Hall, J. E., Accumulation and intracellular distribution of antitrypanosomal diamidine compounds DB75 and DB820 in African trypanosomes. *Antimicrob Agents Chemother* **2006,** *50* (6), 2185-91.

29. Rettig, M.; Kamal, A.; Ramu, R.; Mikolajczak, J.; Weisz, K., Spectroscopic and calorimetric studies on the DNA recognition of pyrrolo[2,1-c][1,4]benzodiazepine hybrids. *Bioorg Med Chem* **2009,** *17* (2), 919-28.

30. Harris, D. C., *Quantitative chemical analysis*. 7th ed.; W.H. Freeman and Co.: New York, NY, 2007.

31. Degtyareva, N. N.; Wallace, B. D.; Bryant, A. R.; Loo, K. M.; Petty, J. T., Hydration changes accompanying the binding of minor groove ligands with DNA. *Biophys J* **2007,** *92* (3), 959-65.

32. Brooks, B. E.; Piro, K. M.; Brennan, R. G., Multidrug-binding transcription factor QacR binds the bivalent aromatic diamidines DB75 and DB359 in multiple positions. *J Am Chem Soc* **2007,** *129* (26), 8389-95.

33. Gaigalas, A. K.; Li, L.; Henderson, O.; Vogt, R.; Barr, J.; Marti, G.; Weaver, J.; Schwartz, A., The development of fluorescence intensity standards. *J Res Natl Inst Stan* **2001,** *106* (2), 381-389.

34. Vazquez, O.; Sanchez, M. I.; Martinez-Costas, J.; Vazquez, M. E.; Mascarenas, J. L., Bis-4-aminobenzamidines: versatile, fluorogenic A/T-selective dsDNA binders. *Org Lett* **2010,** *12* (2), 216-9.

35. Ladbury, J. E.; Doyle, M. L., *Biocalorimetry 2 : applications of calorimetry in the biological sciences*. Wiley: Chichester ; Hoboken, NJ, 2004; p xv, 259 p.

36. Suchetan, P. A.; Gowda, B. T.; Foro, S.; Fuess, H., 4-Methyl-N-(4-methyl-benzo-yl)benzene-sulfonamide. *Acta Crystallogr Sect E Struct Rep Online* **2010,** *66* (Pt 6), o1510.

37. Mazur, S.; Tanious, F. A.; Ding, D.; Kumar, A.; Boykin, D. W.; Simpson, I. J.; Neidle, S.; Wilson, W. D., A thermodynamic and structural analysis of DNA minor-groove complex formation. *J Mol Biol* **2000,** *300* (2), 321-37.

38. Rohs, R.; West, S. M.; Sosinsky, A.; Liu, P.; Mann, R. S.; Honig, B., The role of DNA shape in protein-DNA recognition. *Nature* **2009,** *461* (7268), 1248-53.

39. Drew, H. R.; Dickerson, R. E., Structure of a B-DNA dodecamer. III. Geometry of hydration. *J Mol Biol* **1981,** *151* (3), 535-56.

40. Shatzky-Schwartz, M.; Arbuckle, N. D.; Eisenstein, M.; Rabinovich, D.; Bareket-Samish, A.; Haran, T. E.; Luisi, B. F.; Shakked, Z., X-ray and solution studies of DNA oligomers and implications for the structural basis of A-tract-dependent curvature. *J Mol Biol* **1997,** *267* (3), 595-623.

41. Spolar, R. S.; Livingstone, J. R.; Record, M. T., Jr., Use of liquid hydrocarbon and amide transfer data to estimate contributions to thermodynamic functions of protein folding from the removal of nonpolar and polar surface from water. *Biochemistry* **1992,** *31* (16), 3947-55.

42. Spolar, R. S.; Record, M. T., Jr., Coupling of local folding to site-specific binding of proteins to DNA. *Science* **1994,** *263* (5148), 777-84.

43. Freire, E.; Murphy, K. P.; Sanchez-Ruiz, J. M.; Galisteo, M. L.; Privalov, P. L., The molecular basis of cooperativity in protein folding. Thermodynamic dissection of interdomain interactions in phosphoglycerate kinase. *Biochemistry* **1992,** *31* (1), 250-6.

7 Appendix

7.1 Derivation of Equations 2.3 and 2.4

For a single site binding model, the equilibrium can be described by:

where M is the free DNA, L is the free ligand and ML is the ligand-DNA complex. From this equilibrium, an equilibrium binding constant can be determined:

where K is the equilibrium binding constant. Assuming that only L and ML show fluorescence, since DNA does not fluoresce, and that their fluorescence intensities differ, a fraction of complex can be determined by:

where X_{ML} is the fraction of the complex, F is the observed fluorescence, F_0 is the fluorescence of the free ligand, and F_∞ is the fluorescence of the ligand-DNA complex. By replacing ML using equation 2:

To normalize the data, expand equation 3 b by the fraction ― and replacing fluorescence by molar fluorescence:

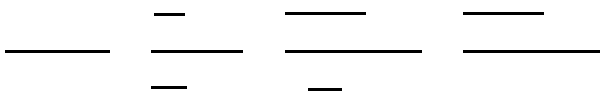

Where L_0 is the total concentration of the ligand, is the molar fluorescence of the free ligand, is the molar fluorescence of the ligand-DNA complex and ― is the fluorescence enhancement factor. If fluorescence decreases upon binding the enhancement factor will be less than 1 and if the fluorescence increases upon binding the enhancement factor will be greater than 1. The final relation for the fraction of the complex is:

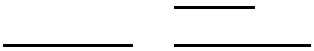

By rearranging 3 d, we get:

To calculate the concentration of free DNA [M] as a function of the L_0 (total concentration of the ligand), M_0 (total concentration of the DNA) and K (equilibrium binding constant), we use the following equations:

By combining equations 2, 5 and 6:

Rearranging equation 7:

By solving the quadratic equation in equation 8:

Finally by replacing [M] in equation 4 by equation 9:

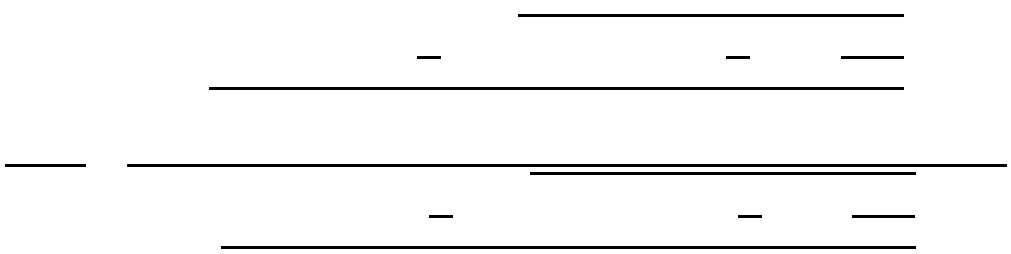

To determine K, plot the normalized fluorescence versus the DNA concentration and perform a non-linear least squares regression with K and η as fitting parameters.

7.2 Detailed ITC Procedure

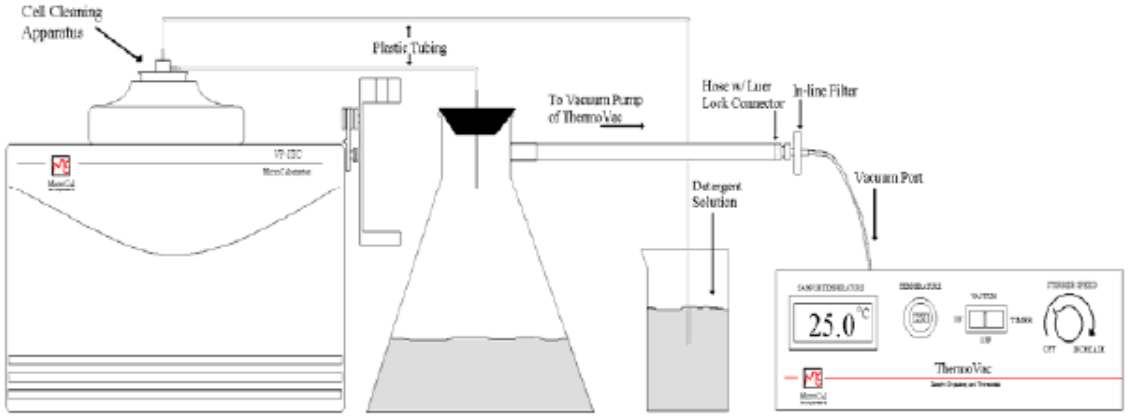

Figure 1: ITC sample cell cleaning setup

7.2.1 **Cleaning ITC Sample Cell with ThermoVac**

Insert the cell cleaning apparatus into the adapter, until the top flange is touching the top of the adapter. *(This is generally left put together.)* Referring to Figure1, remove the cap of the ITC to insert the long needle of the cleaning apparatus into the sample cell and push down carefully until the o-ring has sealed. The end of the plastic tubing from the upper tube of the cell cleaning apparatus is immersed into a beaker of 700 mL of 2.5% Contrad 70 detergent solution. ***(Only use a basic solution, not acid as it will damage the cell.)*** The end of the plastic tubing from the lower tube of the cell is connected to a 1L vacuum flask through the #8 stopper. Attach the side arm of the flask to the vacuum port of the ThermoVac. Turn on the ThermoVac vacuum pump. This will pull the detergent from the beaker, through the cell and into the waste flask. ***(Make sure not to allow the flask to fill up too close to the side arm as it will be sucked into the ThermoVac system and damage it.)*** Once the detergent has been passed through the cell, repeat the procedure with deionized water. Once the vacuum has had sufficient time to pull all the liquid from the cell into the waste flask, turn off the vacuum pump and remove the

cleaning apparatus. Remove any remaining water from the cell with a long needle syringe. Replace the cap of the ITC instrument. *(This prevents unwanted debris in the cell.)* This process will take approximately **2 hours**.

Critical Points Summary

- Only use a basic solution, NEVER an acid solution as it will damage the cell
- Make sure to carefully watch the apparatus to make sure nothing gets sucked into the ThermoVac system
- Make sure that there is 2 hours of time available to complete this process

7.2.2 Cleaning ITC Injection Syringe

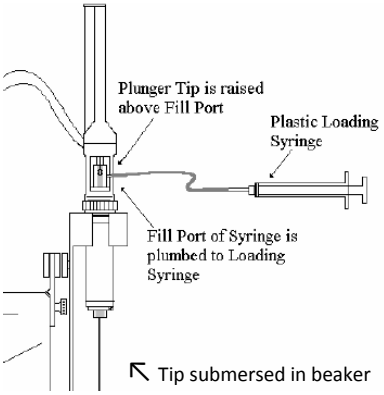

Figure 2: ITC injection syringe schematic

Care should be taken not to bend the expensive syringe needle, as it will **damage** the functionality of the instrument, since the syringe spins during the experiment. Leaving the syringe in the auto pipette, attach the plastic tubing of the loading syringe to the filling port of the syringe, see Figure 2. Open the VPViewer 2000 software, click on the "Open Fill Port" button to open the fill port, see Figure 3. Insert the tip of the syringe into a beaker of deionized water. Using the loading syringe pull 30-50 mL of the deionized water through the syringe. Repeat with 2.5% Contrad 70 detergent solution. Repeat with deionized water. Remove syringe from beaker, then pull any

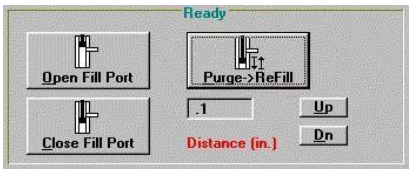

Figure 3: VPViewer controls for syringe

remaining liquid through the syringe, so as not to dilute the next sample. Click on the "Close Fill Port" button to close the fill port. Remove the plastic tubing of the loading syringe from the injection syringe.

7.2.3 ITC Experimental Procedure

(Procedure based on VP-ITC MicroCalorimeter User's Manual)

VPC-ITC instrument should be thoroughly cleaned prior to any experiment to prevent any unwanted interactions from previous experiments.

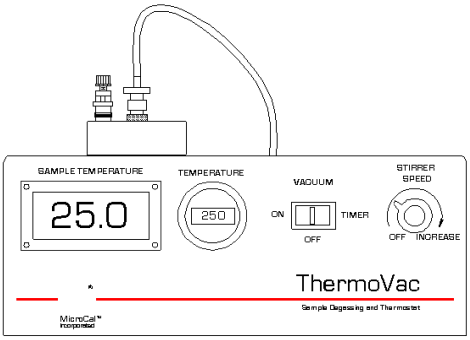

Figure 4: Schematic of ThermoVac

Degassing prevents any unwanted gas bubbles from interfering with the heat measurement in the experiment. The buffer was degassed by being placed into three small plastic vials, which are specially fitted to the ThermoVac, with a small stir bar, see Figures 4 and 5. The sample temperature is set to 25 ^{o}C. The vials are placed in the tube holder for 30 minutes covered by the vacuum cap while being stirred. One vial will be used for the reference cell in VP-ITC instrument, one vial for the DNA preparation, and one vial for the ligand preparation. Alternatively, the samples may be prepared, then degassed; however, be careful that there is no evaporation as this will alter the molarity of the solution. Once degassing is complete, release the pressure by opening the bleeder valve.

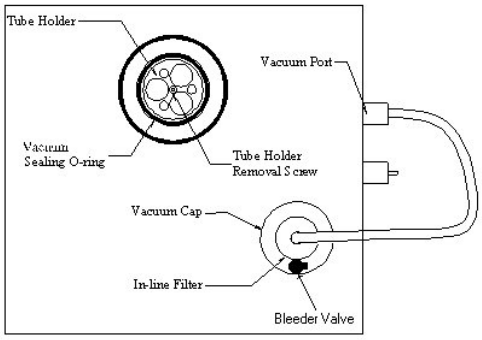

Figure 5: Top view of ThermoVac

While the buffer is degassing, rinse the sample cell and the auto-pipette injection syringe with the same buffer that will be used for the experiment. Rinse the sample cell twice with the buffer using the long needle syringe. Make sure to remove as much liquid as possible, as it can dilute the sample. To rinse the injection syringe, click on the "Open Fill Port" button to open the fill port. Insert the tip of the syringe into a beaker of buffer. Using the loading syringe pull 15 mL of the buffer through the syringe to rinse. Remove syringe from beaker, then pull any remaining liquid through the syringe, so as not to dilute the sample. Click on the "Close Fill Port" button to close the fill port. Remove the plastic tubing of the loading syringe from the injection syringe.

Once the buffer is degassed, prepare the DNA and the ligand for the experiment. Make sure to label all vials to avoid confusion. Prepare 2500 µL of 0.01 mM DNA in a small plastic vial. Prepare 3000 µL of 0.10 mM ligand in a small plastic vial. (Actual molarities may vary generally ligand 10X the molarity of the DNA.)

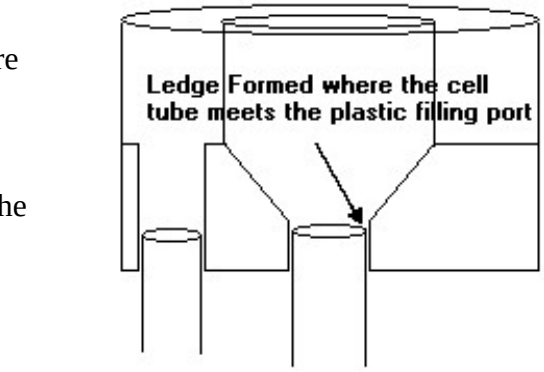

Figure 6: Schematic of reference cell and sample cell from the side.

The remaining degassed buffer was placed in the reference cell of the VP-ITC. Remove the cap from the top of the instrument to access the reference cell, see Figure 6. Twist the reference plug assembly into the cap of the reference cell and pull up to remove cap, see Figure 7. Fill up the long needle syringe with a minimum of 1.8 mL of degassed buffer. Make sure to remove all air bubbles from the syringe. Slowly fill up the reference cell until it is completely full. Make sure to

Figure 7: Reference plug assembly

remove any excess liquid that overflows from the cell using the long needle syringe. Replace the cap on the reference cell by pushing it into the cell and untwisting the reference plug assembly to remove it from the reference cell cap.

Fill the long needle syringe with a minimum of 1.8 mL of the DNA to add to the sample cell. When inserting the needle into the cell, insert it ***very slowly and carefully*** keeping it in an upright position. Once the needle gently touches the bottom of the cell, raise the needle approximately 1 mm off the bottom of the cell. The syringe should not be moved during the filling process. ***Slowly*** inject the DNA solution so that it fills up the cell and spills out the top of the cell stem. Carefully remove any excess solution outside of the cell by place the tip of the needle on the ledge. Make sure not to remove any solution from the actual sample cell. Replace cap on the top of the instrument.

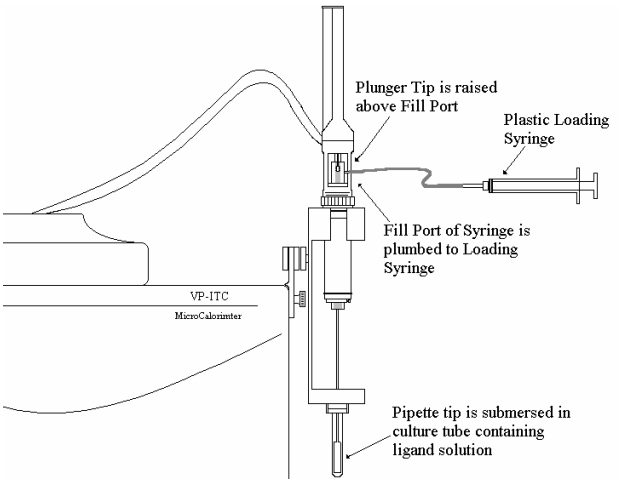

Figure 8: Schematic of auto-pipette injection syringe loading

Submerse the injection syringe needle in the small plastic vial with the 0.10 mM ligand solution; secure the vial in the pipette holder, see Figure 8. Leaving the auto-pipette in the holder, attach the plastic tubing of the loading syringe to the filling port of the injection syringe. Click on the "Open Fill Port" button to open the fill port. Using the loading syringe, slowly pull

the plunger to draw ligand solution into the injection syringe. ***Make sure the auto-pipette injection syringe stays upright and submerged when filling***. Once the bubble passes through the plastic tube of the loading syringe, which is connected at the fill port, click on the "Close Fill Port" button to close the fill port. Remove the plastic tubing of the loading syringe from the injection syringe. Click on the "Purge→Refill" button to purge and refill the syringe to dislodge and eliminate any air bubbles; do this three times. ***Extreme care should be taken to place the auto-pipette injection syringe into the sample cell without causing any air bubbles and minimal disturbance in the sample cell.*** Remove the cap of the ITC instrument. Carefully remove the auto-pipette from the holder. Keep the auto-pipette in the upright position to load it into the sample cell. Very, very slowly insert the injection syringe into the sample cell. Once the injection syringe is in the sample cell, push down carefully to seat the syringe until the o-ring has sealed.

The VPViewer 2000 software is used to choose the run parameters of the experiment, see Figure 9.

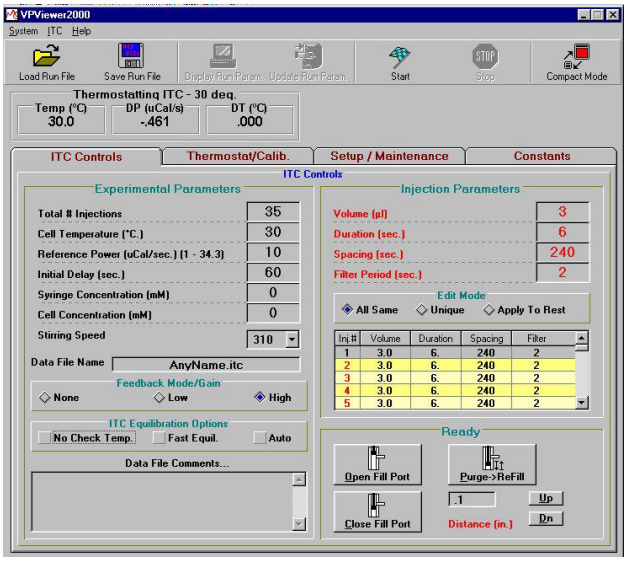

Figure 9: VPViewer software parameters screen
Note: Picture does not show correct run parameters, it is for reference the location of the parameters.

Experimental Parameters (in general)

- Total Injections: 30
- Cell Temperature (C^o): 25
- Reference Power (µcal/sec): 1
- Initial Delay (sec): 300
- Syringe Concentration (mM): 0.10
- Cell Concentration (mM): 0.01
- Stirring Speed: 290
- Data File Name: *Filename*.itc

  (Filename may have up to 16 characters. Do not start with a number. Do not include hyphens, periods or spaces in name. Make sure to check "SETUP/MAINTENANCE" tab to verify path where the file is being saved.)

Feedback Mode/Gain

- Check the box for High

ITC Equilibrium Options

- Check the box for Fast
- Check the box for Auto

Injection Parameters (for 1st injection are different from the rest)

- Volume (µL): 2
- Duration (sec): 4
- Spacing (sec): 300
- Filter Period (sec): 1

Click on "Inj # 2" line below the Edit Mode box. Go back to the injection parameters and update the parameters for the rest of the injections.

Injection Parameters (for remaining injections)

- Volume (µL): 10
- Duration (sec): 20
- Spacing (sec): 300
- Filter Period (sec): 1

Once the parameters for injections 2-30 are input, check off the "Apply to Rest" box in the Edit Mode box. *Note: If the Thermostatting Temperature is higher than the experimental parameter, the instrument will have to actively cool and reheat the jacket before starting the experiment.* Once all parameters have been set and rechecked; click on the "Start" button to run the experiment. From this point until completion of the experiment the instrument will not need any adjustment, it will run on its own. This will take approximately 3 hours. However, the experiment can be monitored as it progresses.

At the start of the experiment the instrument may rapidly bypass certain stages of operation. Just prior to the start of the actual experimental procedure the Microcal Origin will display that it is in "Final Baseline Equilibration" in red in the upper right hand corner of the screen, see Figure 10. Once this begins, the injection syringe starts stirring and applies power to the reference cell. The next step will be "Pre-Titration Delay and the volume remaining in the syringe". Once the injections begin, it will read "ITC Injection #X, X µL Available"; this way progress can be monitored. Once it has completed all the injections, it will read "Thermostatting ITC @ 25°C", see Figure 11.

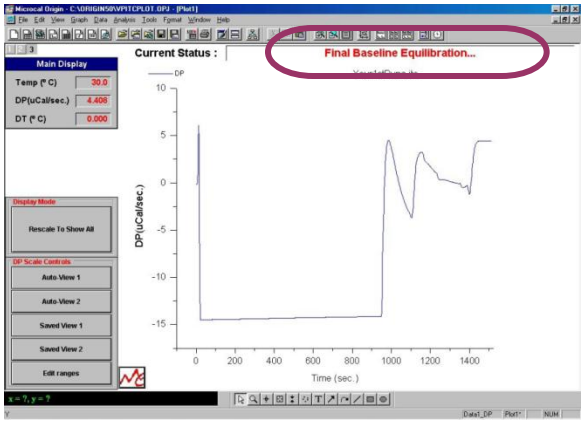

Figure 10: Origin software screen for tracking the experiment progress
Note: Picture does not show correct run parameters, it is for reference the location of the current step of the experiment.

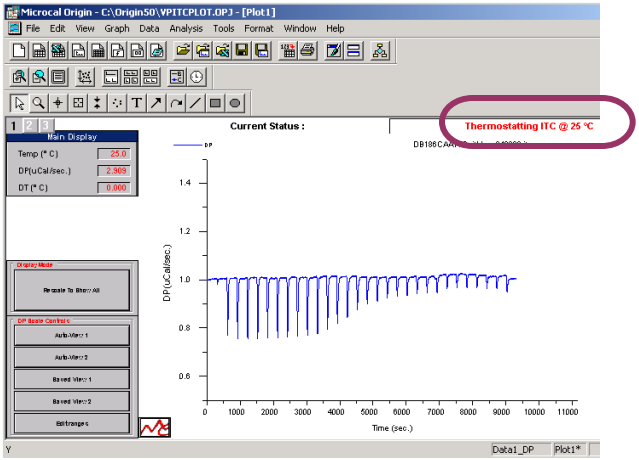

Figure 11: Screen view when experiment has completed.
Note: Picture does not show correct run parameters, it is for reference the location of the current step of the experiment.

Repeat entire procedure for baseline adjustment data, with the following alteration: in the sample cell use buffer only, with no DNA. This will be used to adjust results for the ligand interaction with the buffer.

7.2.4 **Data Analysis for ITC**

To open Origin 7 for the ITC application for data analysis click on icon for Microcal LLC, ITC icon. On the main screen there will be four buttons in the ITC Main Control box; click on the "Read Data" button to browse for the data file for the experiment. *(If you do not see this box, it is not the right software icon.)* Once you have selected the file it will be displayed on the screen, see Figure 12. ***(Save the project periodically to not lose progress, original data file will not be altered by saving the project. To re-open project, click on "File" on the upper tool bar and select "Open", the file will have an .OPJ file type)*** The integration needs to be adjusted to compensate for any tailing or baseline noise. This is evident in the scattering of the points on the "Delta H" screen, see Figure 13.

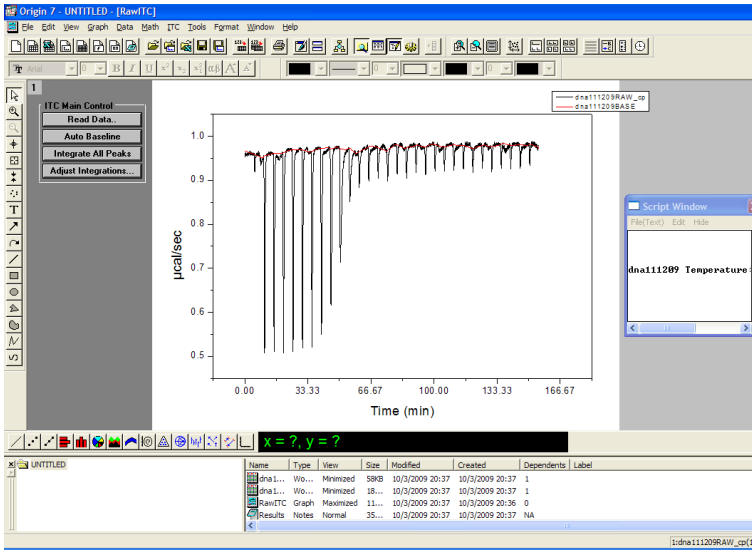

Note: To switch screens within Origin 7 click on the appropriate file name in the box in the lower right hand of the screen.
←

Figure 12: Origin 7 for ITC "Raw Data" screen layout prior to integration adjustment.

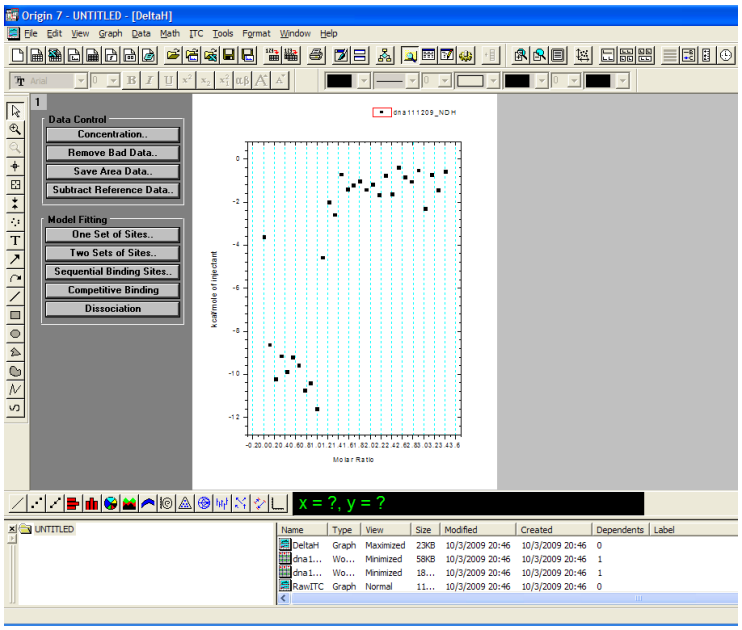

Figure 13: Delta H screen layout prior integration adjustment.

To adjust the baseline, click on the "Adjust Integration" button in the ITC Main Control Box on the "Raw Data" screen. The screen will change to the "Adjust Integration" screen to adjust the actual baseline, which will alter the integration. Figure 14A shows what the baseline looked like prior to adjustment, while Figure 14B shows what the baseline looked like after the adjustment. The goal is for the integration area to be accurate for just the main peak, not the additional noise, so even out the excess integration above and below the baseline. To adjust the baseline, click on the "Baseline" button. The baseline will then have squares on it that can be moved by clicking the square with the mouse and dragging them to the appropriate spot. *Note: To make it easier to see the actual changes in the "Delta H" screen, have the "Delta H" and "Adjust Integration" screens both visible at the same time, see Figure 15.* Once you have moved the baseline, click on the "Integrate" button to view the integration and see if it appears to actual balance out the noise. *This can be refined more than once, and may need to refined more*

than once as the baseline adjustment progresses. Once the particular peak has been adjusted the forward arrows "›› " will advance one peak to the right and the backward arrow "‹‹" will advance one peak to left. Once complete, click "Quit" to return to the "Raw Data" screen.

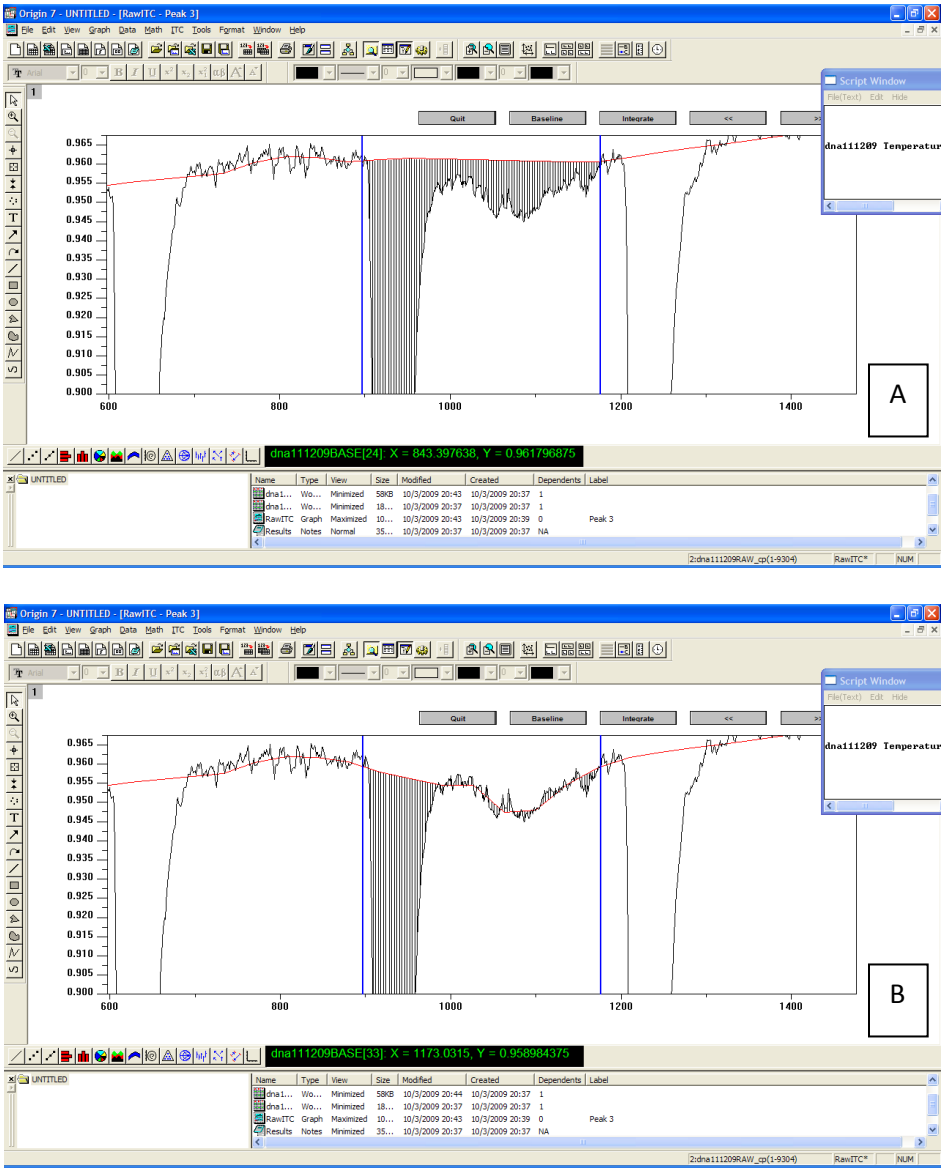

Note: Scale may be adjusted for a better view by double clicking on y-axis. A new screen will appear. Make sure the "Scale" tab is displayed, select a "From" and "To" to better suit display needs. Change "Rescale" option to "Manual", so that it does not rescale when frames are shifted.

Figure 14: "Adjust Integration" screen: A.) prior to adjustment of baseline. B.) after baseline adjustment.

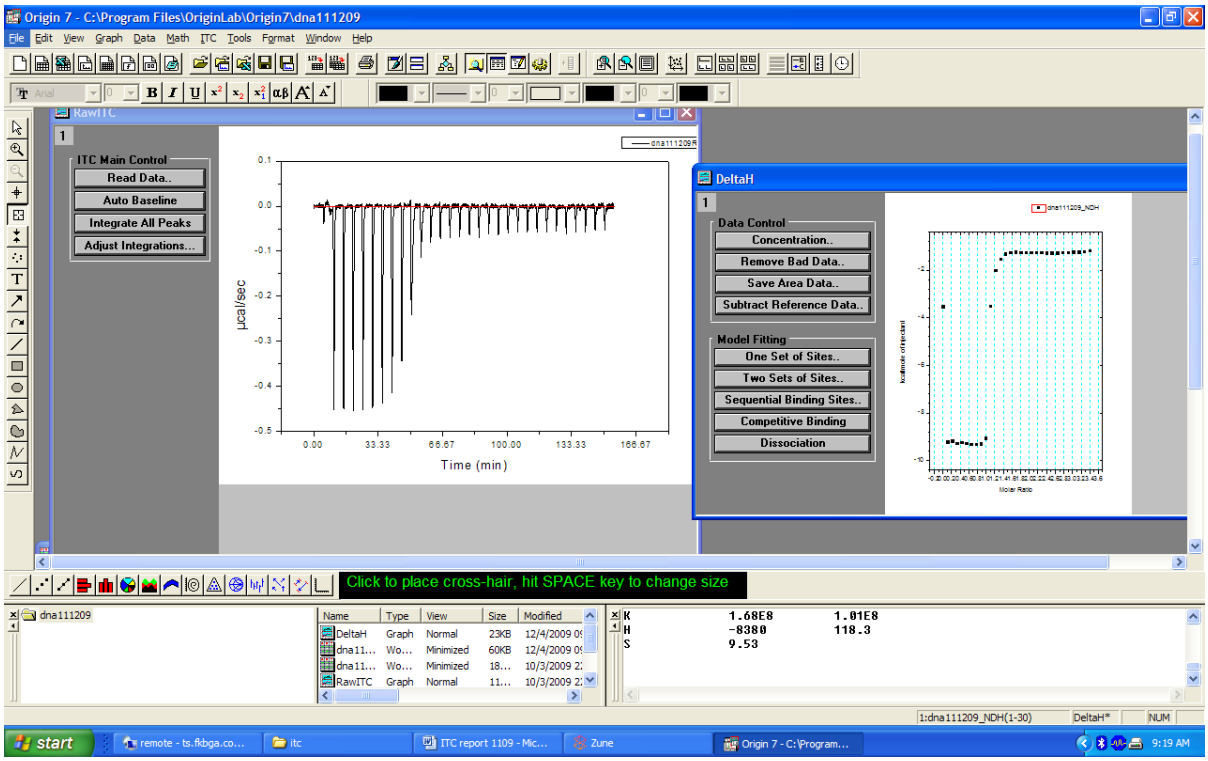

Figure 15: "Raw Data" and "Delta H" screens after adjustment of baseline.

Once the integration adjustment is complete maximize the "Delta H" screen. To check that the concentration values are correct for the syringe and cell, click on the "Concentration" button in the Data Control box, see Figure 16. *(If actual concentrations are in question, they should be checked by UV-Vis Spectroscopy.)* Click "OK" to return to "Delta H" screen.

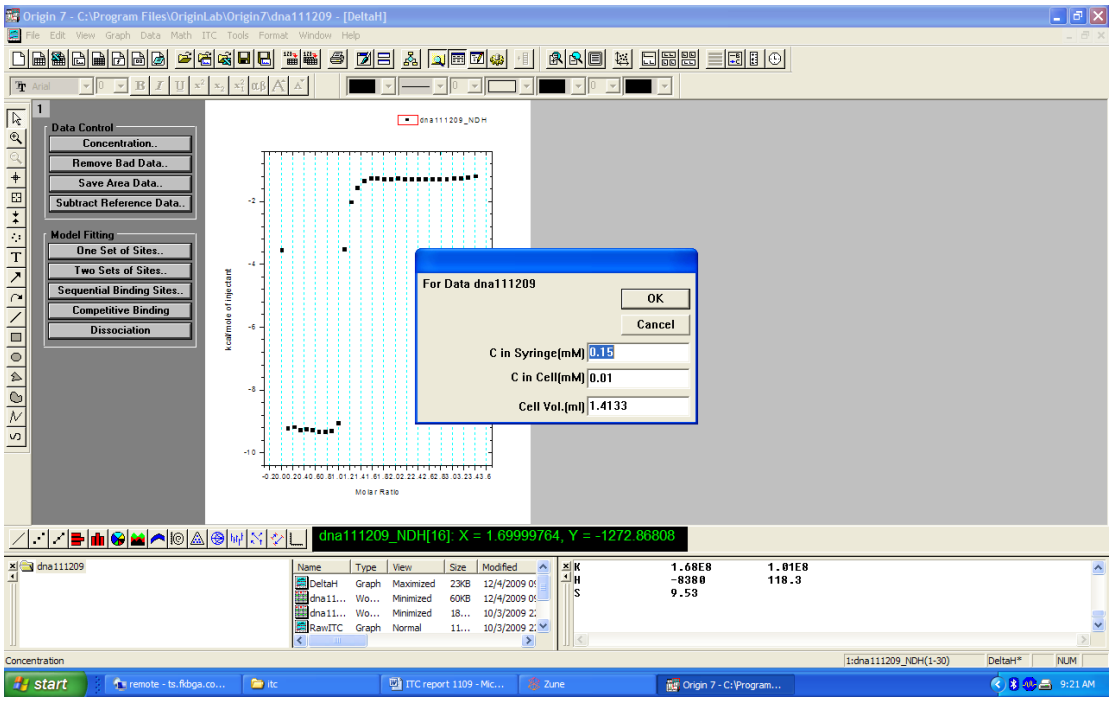

Figure 16: Concentration information from "Delta H" screen.

The next step is to remove bad data points, this should be limited. The first injection will always be a bad data point, which is why it is a smaller injection than the rest of the injections. To remove a bad data point, click on "Remove Bad Data". The cross hairs will appear on the screen, place them over the point to be removed and hit the enter key. *Note: If you re-integrate, or do some other functions after this, the point may come back on the screen, so you may have to perform this step again. Just make sure it is removed prior to model fitting.* The next step is to subtract the baseline reference data. *There are multiple ways to do this, however, simple math was used, see ITC Data Analysis in Origin Tutorial Guide p. 29-42 for alternative method.* To subtract the baseline reference (the ligand interaction with the buffer), click on "Math" in the

upper toolbar, then select “Simple Math” (see Figure 17). The average response for the reference is keyed as calories, not kcal, so if the response was -.990 kcal, then the proper operator is a “+” *(a negative, negative is a positive)* 990 cal. *Note: This should generally make the upper portion of the graph line up with 0 kcal/mol of injectant on the y-axis.* Then click “OK” to return to the “Delta H” screen.

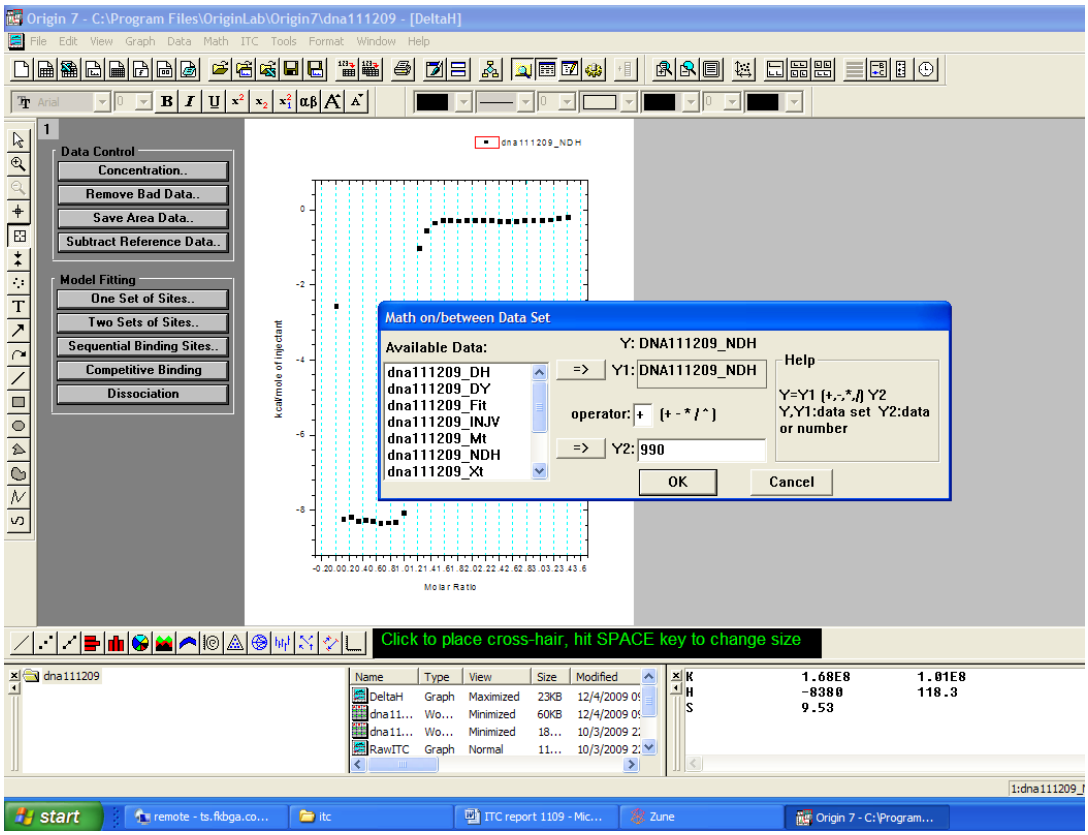

Figure 17: “Simple Math” screen layout.

The next step is to fit the curve by "Model Fitting". For this experiment, one set of binding sites is the appropriate choice; therefore click on "One Set of Sites" button in the Model Fitting box (see Figure 18). To fit the curve, choose the "100 Iter" button. This will do 100 iterations of fitting the curve. Once fitting is completed click on "Done" button to return to the "Delta H" screen. A red line will now be fitted to the curve and a dialog box will appear displaying the results of the experiment, see Figure 19.

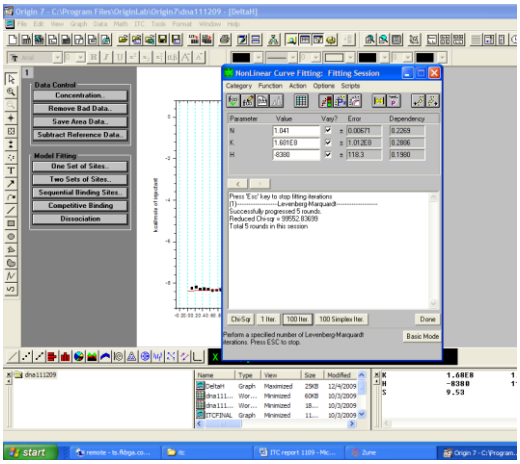

Figure 18: Model fitting for one set of sites.

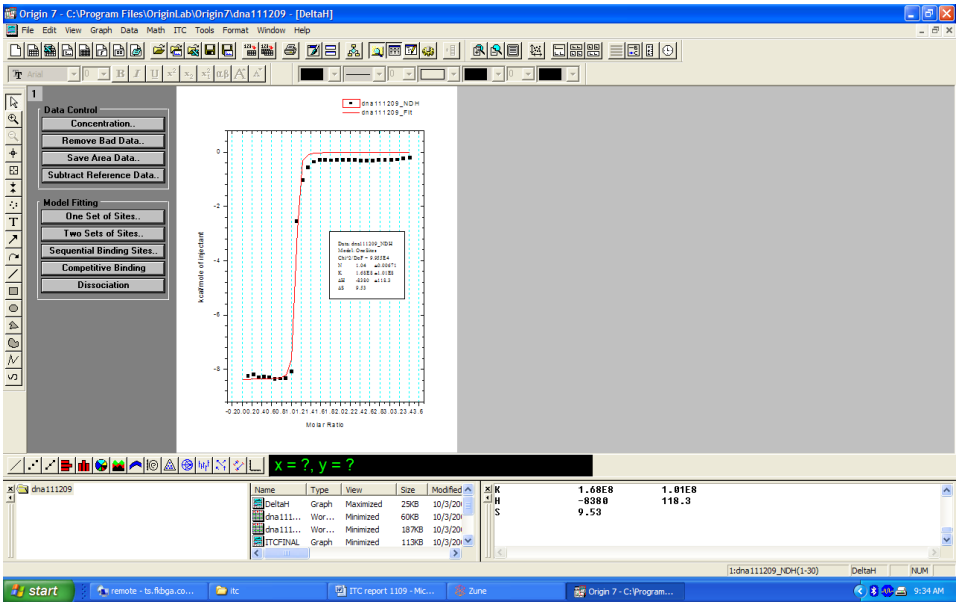

Figure 19: "Delta H" screen after model fitting for one set of sites, with results box displayed.

The last step in Data Analysis is to prepare the Final Figure for use in publication. On the "Delta H" screen, click on "ITC" in the upper tool bar, then select Final Figure. The Final Figure will appear, see Figure 20.

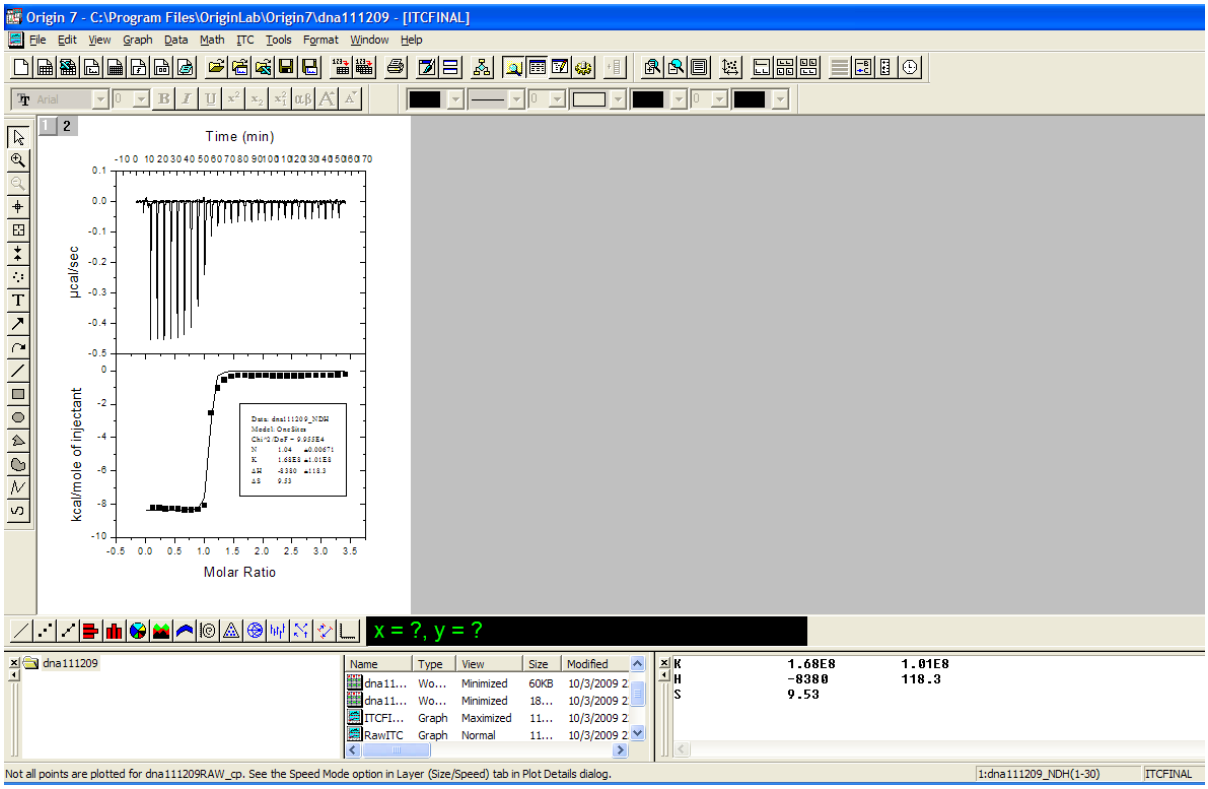

Figure 20: "Final Figure" created upon completion of data analysis.